



ARISTOTLE UNIVERSITY OF THESSALONIKI  
Interinstitutional Program of Postgraduate Studies in  
PALAEOLOGY – GEOBIOLOGY



MICHAILIDIS IOANNIS  
Geologist

NANNOFOSSIL BIOSTRATIGRAPHY OF THE PALEOGENE  
MOLASSIC DEPOSITS OF WESTERN THRACE BASIN

MASTER THESIS

*DIRECTION: Micropalaeontology – Biostratigraphy*  
*Directed by: National & Kapodistrian University of Athens*



ATHENS  
2020





Interinstitutional  
Program of  
Postgraduate  
Studies in  
PALAEOLOGY – GEOBIOLOGY

supported by:



Τμήμα Γεωλογίας ΑΠΘ  
School of Geology AUTH



school of biology

Τμήμα Βιολογίας ΑΠΘ  
School of Biology AUTH



**National and  
Kapodistrian  
University of  
Athens**  
Faculty of Geology  
and Geoenvironment

Τμήμα Γεωλογίας & Γεωπεριβάλλοντος  
ΕΚΠΑ  
Faculty of Geology & Geoenvironment  
NKUA



Τμήμα Γεωλογίας Παν/μίου Πατρών  
Department of Geology, Patras Univ.



UNIVERSITY OF THE AEGEAN

Τμήμα Γεωγραφίας Παν/μίου Αιγαίου  
Department of Geography, Aegean Univ.





MICHAILIDIS IOANNIS  
ΜΙΧΑΗΛΙΔΗΣ ΙΩΑΝΝΗΣ  
Πτυχιούχος Γεωλογίας

NANNOFOSSIL BIOSTRATIGRAPHY OF THE PALEOGENE  
MOLASSIC DEPOSITS OF WESTERN THRACE BASIN

ΒΙΟΣΤΡΩΜΑΤΟΓΡΑΦΙΑ NANNOΑΠΟΛΙΘΩΜΑΤΩΝ ΤΩΝ  
ΠΑΛΑΙΟΓΕΝΩΝ ΜΟΛΑΣΣΙΚΩΝ ΑΠΟΘΕΣΕΩΝ ΤΗΣ ΔΥΤΙΚΗΣ  
ΛΕΚΑΝΗΣ ΤΗΣ ΘΡΑΚΗΣ

Υποβλήθηκε στο ΔΠΜΣ Παλαιοντολογία-Γεωβιολογία

Ημερομηνία Προφορικής Εξέτασης: 23/12/2020  
Oral Examination Date: 23/12/2020

**Three-member Examining Board**

Professor Triantaphyllou Maria, Supervisor (NKUA)  
Professor Dimiza Margarita, Member (NKUA)  
Associate Professor Koukousioura Olga, Member (AUTH)

**Τριμελής Εξεταστική Επιτροπή**

Καθηγήτρια Τριανταφύλλου Μαρία, Επιβλέπων (ΕΚΠΑ)  
Επίκουρη καθηγήτρια Δήμιζα Μαργαρίτα, Μέλος Τριμελούς Εξεταστικής Επιτροπής (ΕΚΠΑ)  
Αναπληρώτρια Καθηγήτρια Κουκουσιούρα Όλγα, Μέλος Τριμελούς Εξεταστικής Επιτροπής (ΑΠΘ)



© Michailidis Ioannis, Geologist, 2020

All rights reserved.

NANNOFOSSIL BIOSTRATIGRAPHY OF THE PALEOGENE MOLASSIC DEPOSITS OF WESTERN THRACE BASIN – *Master Thesis*

© Μιχαηλίδης Ιωάννης, Γεωλόγος, 2020

Με επιφύλαξη παντός δικαιώματος.

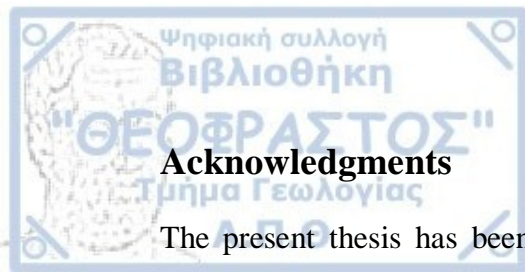
ΒΙΟΣΤΡΩΜΑΤΟΓΡΑΦΙΑ ΝΑΝΝΟΑΠΟΛΙΘΩΜΑΤΩΝ ΤΩΝ ΠΑΛΑΙΟΓΕΝΩΝ ΜΟΛΑΣΣΙΚΩΝ ΑΠΟΘΕΣΕΩΝ ΤΗΣ ΔΥΤΙΚΗΣ ΛΕΚΑΝΗΣ ΤΗΣ ΘΡΑΚΗΣ  
– *Μεταπτυχιακή Διπλωματική Εργασία*

Citation:

Michailidis, I., 2020. – Nannofossil biostratigraphy of the Paleogene molassic deposits of Western Thrace Basin. Master Thesis, Interinstitutional Program of Postgraduate Studies in Palaeontology-Geobiology. School of Geology, Aristotle University of Thessaloniki, 85 pp.

It is forbidden to copy, store and distribute this work, in whole or in part, for commercial purposes. Reproduction, storage and distribution are permitted for non-profit, educational or research purposes, provided the source of origin is indicated. Questions concerning the use of work for profit-making purposes should be addressed to the author.

The views and conclusions contained in this document express the author and should not be interpreted as expressing the official positions of the Aristotle University of Thessaloniki.



## Acknowledgments

The present thesis has been realized within the framework of the Interinstitutional Program of Postgraduate Studies in Palaeontology – Geobiology and specialization in Micropaleontology – Biostratigraphy. All laboratory procedures such as preparation and analysis of samples were carried out in the facilities of the Department of Historical Geology and Paleontology of the National and Kapodistrian University of Athens.

First and foremost I would like to express my deep and sincere gratitude to my supervisor Dr. Triantaphyllou Maria, for assigning me this fascinating project as well as for her guiding, tutoring and constant feedback during all stages of this research.

Special thanks to Dr. Papanikolaou Dimitrios who along with Dr. Triantaphyllou Maria performed the sampling process of the study area and provided me with the samples.

I am also extremely thankful to the rest of my committee Dr. Dimiza Margarita and Dr. Koukousioura Olga for providing me with invaluable learning opportunities and notes.

Finally, I couldn't thank enough my parents and my sister. Their unceasing support and encouragement, throughout the years of my studies, helped me stay focused until the completion of my research without getting overwhelmed by the rough times that came by.



## Abstract

The Thrace basin is one of the largest and most important basins in the North Aegean region. The eastern part of this basin extends to NW Turkey and has been extensively studied due to its high hydrocarbon potential. The western basin of Thrace is located in NE Greece and is the study area of the present work. It belongs to the Rhodope – North Aegean molassic basin and is characterized by Paleogene molassic deposits that are marginalized in the NW part by the metamorphic rocks of the Rhodope massif. Papanikolaou & Triantafyllou (2010) identified two fault zones (FZ), the Ardas FZ and Soufli FZ, which divide the Western Thrace basin into three sub-basins (SB), Petrota SB in the North, the Alexandroupolis SB in the South and the Orestias SB between the other two. The most complete sequence of the molassic formations is observed in the Alexandroupolis SB. As part of this research, sampling of the formations of the Alexandroupolis SB was carried out, during which, 44 samples were collected from natural and artificial outcrops. From these samples, 51 smear slides were created and studied for their content in calcareous nannofossils, using a semi-quantitative analysis under polarizing light microscope. Out of the 44 samples, 11 contained nannofossils. These were identified and the percentage of participation of each species in the samples was determined. Despite the low preservation and content of nannofossils, with the presence of index species, such as *Isthmolithus recurvus*, *Sphenolithus predistentus*, *S. distentus*, *S. ciperoensis*, etc., it was possible to achieve the biostratigraphical characterization of the samples. In this way, most of the samples studied were classified in a specific biozone based on the biozonations proposed by Martini (1971) and Agnini et al. (2014) defining, finally, a more detailed dating of the molassic sediments that comprise the Western Thrace basin.



## Περίληψη

Η λεκάνη της Θράκης αποτελεί μία από τις μεγαλύτερες και σημαντικότερες λεκάνες στην ευρύτερη περιοχή του Βόρειου Αιγαίου. Το ανατολικό μέρος της λεκάνης αυτής εκτείνεται στην ΒΔ Τουρκία και έχει μελετηθεί εκτενώς λόγω της μεγάλης πιθανότητας υδρογονανθράκων. Η Δυτική λεκάνη της Θράκης τοποθετείται στην ΒΑ Ελλάδα και είναι η περιοχή μελέτης της παρούσας εργασίας. Ανήκει στην μολασσική λεκάνη της Ροδόπης - Βορείου Αιγαίου και χαρακτηρίζεται από Παλαιογενείς μολασσικές αποθέσεις που περικλείονται στο ΒΔ τμήμα από τα μεταμορφωμένα πετρώματα της μάζας της Ροδόπης. Οι Παπανικολάου & Τριανταφύλλου (2010) αναγνώρισαν δύο ρηγματογενείς ζώνες (PZ), την PZ του Αρδά και την PZ του Σουφλίου, οι οποίες διαιρούν την Δυτική λεκάνη της Θράκης σε τρεις επιμέρους υπολεκάνες (ΥΛ), την ΥΛ των Πετρωτών στον Βορρά, την ΥΛ της Αλεξανδρούπολης στο Νότο και την ΥΛ της Ορεστιάδας ενδιάμεσα των άλλων δύο. Στην ΥΛ της Αλεξανδρούπολης παρατηρείται η πιο πλήρης ακολουθία των μολασσικών σχηματισμών. Στα πλαίσια αυτής της έρευνας πραγματοποιήθηκε δειγματοληψία των σχηματισμών της ΥΛ της Αλεξανδρούπολης κατά την οποία συλλέχθηκαν 44 δείγματα από φυσικές και τεχνητές τομές. Από αυτά τα δείγματα κατασκευάστηκαν 51 αντικειμενοφόρες πλάκες οι οποίες μελετήθηκαν για το περιεχόμενο τους σε ασβεστολιθικά ναννοαπολιθώματα με ημι-ποσοτική ανάλυση κάτω από πολωτικό μικροσκόπιο. Από τα 44 δείγματα, 11 περιείχαν ναννοαπολιθώματα, τα οποία αναγνωρίστηκαν και προσδιορίστηκε το ποσοστό συμμετοχής του κάθε είδους στα δείγματα. Παρά το χαμηλό ποσοστό διατήρησης και περιεκτικότητας ναννοαπολιθωμάτων, επιτεύχθηκε ο βιοστρωματογραφικός χαρακτηρισμός των δειγμάτων με την παρουσία χαρακτηριστικών ειδών, όπως *Isthmolithus recurvus*, *Sphenolithus predistentus*, *S. distentus*, *S. ciperoensis* κ.α. Με αυτόν τον τρόπο τα περισσότερα δείγματα που μελετήθηκαν κατατάχθηκαν σε μία συγκεκριμένη βιοζώνη με βάση τις βιοζωνώσεις που προτάθηκαν από Martini (1971) και Agnini et al. (2014) προσδιορίζοντας, τελικά, μια πιο λεπτομερή χρονολόγηση των μολασσικών ιζημάτων που συντελούν την Δυτική λεκάνη της Θράκης.



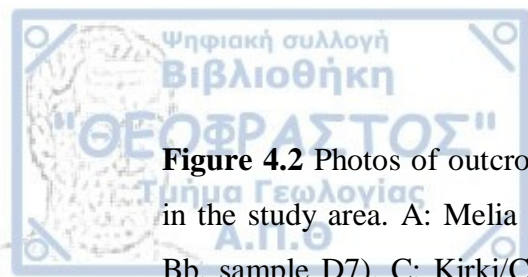
## **Table of contents**

1. Introduction.....	18
1.1 Study Area .....	18
1.2 Scope of this study .....	19
2. Subject of this Study .....	20
2.1 Calcareous Nannoplankton.....	20
2.2 The role of Calcareous Nannoplankton in the marine Carbon cycle .....	22
2.3 Calcareous Nannofossils as tools in Biostratigraphy .....	23
3. Geological Setting .....	27
3.1 The Rhodope – North Aegean Molassic basin .....	30
3.2 Tectonostratigraphy of the Western Thrace basin .....	31
4. Material and Methods.....	35
4.1 Sampling.....	35
4.2 Calcareous nannofossil analysis .....	38
4.2.1 Sample preparation.....	40
4.2.2 Analysis of samples.....	41
5. Results .....	43
5.1 Chorafaki Formation .....	45
5.2 Avas formation.....	47
5.3 Pylaea formation .....	50
6. Discussion / Biostratigraphical characterization.....	68
6.1 Chorafaki formation .....	68
6.2 Avas formation.....	71
6.3 Pylaea formation .....	73
7. Conclusions.....	82
8. References.....	83



## List of figures

<b>Figure 1.1</b> Left: The location of the Thrace basin in the NE Greece. Right: Map by Okay et al. (2019) showing the extent of its sedimentary rocks.....	18
<b>Figure 2.1</b> Schematic representation of (a) the structure and components of a coccolithophore cell and (b) the plan view of a single coccolith under microscope (Source: Bown & Young, 1998) .....	21
<b>Figure 2.2</b> Schematic representation of the Biologic Pump (Ducklow, 2001) .....	22
<b>Figure 2.3</b> Range, Interval and Abundance Zones used in calcareous nannofossil biozonations. (Redrawn by Agnini et al. 2017 after Wade et al., 2011 and Backman et al., 2012).....	24
<b>Figure 2.4</b> Palaeogene calcareous nannofossil biozonations. CP (Okada & Bukry 1980), NP (Martini, 1971), CN (Agnini et al., 2014). On the right, images of CN stage index-species are taken from literature. (* = Base; + = Top; x = crossover) (Agnini et al., 2017) .....	26
<b>Figure 3.1</b> Simplified geological map showing the Thrace basin and the main structural units of the Rhodope and Serbomacedonian massifs with their tectonic relationships, as well as the Sakarya and Strandja metamorphic rocks in northwestern Turkey. (Kiliyas et al., 2013).....	27
<b>Figure 3.2</b> Geological map of Alexandroupolis sheet (H.S.G.M.E., 1977) on the left and Ferai-Peplos-Ainos sheet (H.S.G.M.E., 1980) on the right. ....	28
<b>Figure 3.3</b> Legend of figure 3.2 geological map. ....	29
<b>Figure 3.4</b> The major molassic basins of Greece. 1: Rhodope – North Aegean molassic basin, 2: Mesohellenic molassic Trough, 3: Cretan Sea molassic basin. (Παπανικολάου, 2015) .....	30
<b>Figure 3.5</b> The Western Thrace basin dissected by Ardas and Soufli fault zones into three sub-basins: Orestias SB, Petrota SB and Alexandroupolis SB. (Papanikolaou & Triantaphyllou, 2010).....	32
<b>Figure 3.6</b> Correlated stratigraphic columns of the 3 sub-basins (Petrota SB, Orestias SB and Alexandroupolis SB) that comprise the Western Thrace basin. (Papanikolaou & Triantaphyllou, 2010).....	34
<b>Figure 4.1</b> Lithostratigraphic column of Alexandroupolis sub-basin and the collected samples. (Papanikolaou & Triantaphyllou, 2010).....	36



**Figure 4.2** Photos of outcrops showing the different formations and sampling points in the study area. A: Melia flysch (sample D1). B: Kirki formation (Ba. sample D6, Bb. sample D7). C: Kirki/Chorafaki (sample D15). D: Chorafaki formation (sample D16). E: Avas formation (sample D26) ..... 37

**Figure 4.3** Photos of outcrops showing the different formations and sampling points in the study area. F: Lower Pylaea formation (Fa: sample D28, Fb: sample D27). G: Limestone lentil (sample D24). H: middle/upper Pylaea formation (Ha: sample D17B, Hb: samples D17/D18/D19, Hc: sample D29). ..... 38

**Figure 4.4** Methodology of smear slide preparation for nannofossil analysis under polarized light microscope..... 40

**Figure 4.5** Analysis of smear slides under polarized light microscope ..... 41

**Figure 5.1** The outcrop positions from which the 11 samples that contained calcareous nannofossils were collected. .... 44

**Figure 5.2** Participation percentages of nannofossil species in the whole smear slide of sample D16F. .... 46

**Figure 5.3** Participation percentages of nannofossil species in the whole smear slide of sample D26a. .... 48

**Figure 5.4** Participation percentages of nannofossil species in the whole smear slide of sample D20. .... 52

**Figure 5.5** Participation percentages of nannofossil species in the whole smear slide of sample D24. .... 53

**Figure 5.6** Participation percentages of nannofossil species in the whole smear slide of sample D28B..... 55

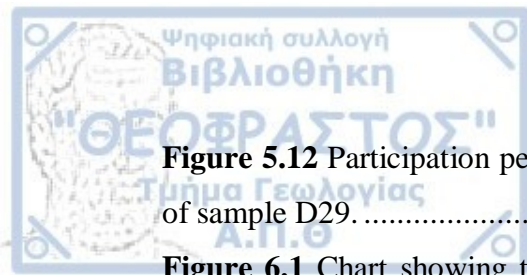
**Figure 5.7** Participation percentages of nannofossil species in the whole smear slide of sample D28a. .... 56

**Figure 5.8** Participation percentages of nannofossil species in the whole smear slide of sample D27. .... 57

**Figure 5.9** Participation percentages of nannofossil species in the whole smear slide of sample D17B..... 58

**Figure 5.10** Participation percentages of nannofossil species in the whole smear slide of sample D18. .... 61

**Figure 5.11** Participation percentages of nannofossil species in the whole smear slide of sample D19. .... 63



**Figure 5.12** Participation percentages of nannofossil species in the whole smear slide of sample D29..... 65

**Figure 6.1** Chart showing the final results and the biostratigraphic interpretation of the samples that contained nannofossils and have been analyzed in this study..... 81



## List of tables

<b>Table 4.1</b>	List of all collected samples and smear slides which were analyzed.....	39
<b>Table 5.1</b>	Species and number of specimens found in 300 FOV in sample D16F. ....	45
<b>Table 5.2</b>	Additional species and number of specimens found in 1500 FOV in sample D16F. ....	46
<b>Table 5.3</b>	Species and number of specimens found in 300 FOV in sample D26a. ....	47
<b>Table 5.4</b>	Additional species and number of specimens found in 1500 FOV in sample D26a. ....	47
<b>Table 5.5</b>	Species and number of specimens found in 300 FOV in sample D20. ....	50
<b>Table 5.6</b>	Additional species and number of specimens found in 1500 FOV in sample D20. ....	51
<b>Table 5.7</b>	Species and number of specimens found in 300 FOV in sample D24. ....	53
<b>Table 5.8</b>	Species and number of specimens found in 300 FOV in sample D28B. ...	55
<b>Table 5.9</b>	Additional species and number of specimens found in 1500 FOV in sample D28B.....	55
<b>Table 5.10</b>	Species and number of specimens found in 300 FOV in sample D28a. ..	56
<b>Table 5.11</b>	Additional species and number of specimens found in 1500 FOV in sample D28a.....	56
<b>Table 5.12</b>	Species and number of specimens found in 300 FOV in sample D27. ....	57
<b>Table 5.13</b>	Additional species and number of specimens found in 1500 FOV in sample D27. ....	57
<b>Table 5.14</b>	Species and number of specimens found in 300 FOV in sample D17B. .	58
<b>Table 5.15</b>	Additional species and number of specimens found in 1500 FOV in sample D17B.....	58
<b>Table 5.16</b>	Species and number of specimens found in 300 FOV in sample D18. ....	60
<b>Table 5.17</b>	Additional species and number of specimens found in 1500 FOV in sample D18. ....	60
<b>Table 5.18</b>	Species and number of specimens found in 300 FOV in sample D19. ....	62
<b>Table 5.19</b>	Additional species and number of specimens found in 1500 FOV in sample D19. ....	62



<b>Table 5.20</b> Species and number of specimens found in 300 FOV in sample D29. ....	64
<b>Table 5.21</b> Additional species and number of specimens found in 1500 FOV in sample D29. ....	64
<b>Table 6.1</b> Calcareous nannofossil distribution for sample D16F based on the semi-quantitative analysis and the biostratigraphical characterization (P: Present, R: Rare, C: Common and RW: Reworked). ....	70
<b>Table 6.2</b> Calcareous nannofossil distribution for sample D26a based on the semi-quantitative analysis and the biostratigraphical characterization (P: Present, R: Rare, C: Common and RW: Reworked). ....	72
<b>Table 6.4</b> Calcareous nannofossil distribution for sample D20 based on the semi-quantitative analysis and the biostratigraphical characterization (P: Present, R: Rare, C: Common and RW: Reworked). ....	74
<b>Table 6.5</b> Calcareous nannofossil distribution for sample D24 based on the semi-quantitative analysis and the biostratigraphical characterization (P: Present, R: Rare, C: Common and RW: Reworked). ....	75
<b>Table 6.3</b> Calcareous nannofossil distribution for samples D28B, D28a, D27 and D17B based on the semi-quantitative analysis and the biostratigraphical characterization (P: Present, R: Rare, C: Common and RW: Reworked). ....	76
<b>Table 6.7</b> Calcareous nannofossil distribution for samples D18 and D19 based on the semi-quantitative analysis and the biostratigraphical characterization (P: Present, R: Rare, C: Common and RW: Reworked). ....	78
<b>Table 6.8</b> Calcareous nannofossil distribution for sample D29 based on the semi-quantitative analysis and the biostratigraphical characterization (P: Present, R: Rare and RW: Reworked). ....	80



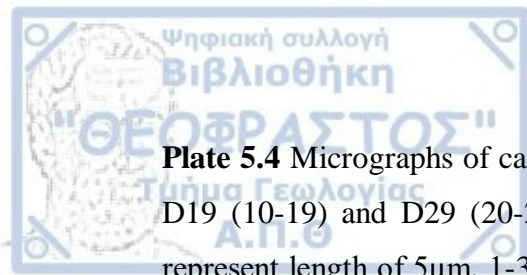
## List of plates

**Plate 5.1** Micrographs of calcareous nannofossil species found in samples D16F (1-17) and D26a (18-31). All scale bars on bottom right of each photograph represent length of 5μm. 1: *Blackites clavus*, 2: *Campylosphaera dela*, 3: *Chiasmolithus nitidus*, 4: *Clausicoccus subdistichus*, 5: *Cribrocentrum reticulatum*, 6: *Discoaster distinctus*, 7: *Ericsonia formosa*, 8: *Micula staurophora*, 9: *Nannoconus funiculus*, 10: *Neococcolithes dubius*, 11: *Pontosphaera obliquipons*, 12: *Reticulofenestra dictyoda*, 13: *Reticulofenestra hillae*, 14: *Reticulofenestra umbilicus*, 15: *Sphenolithus furcatolithoides* "morphotype B", 16: *Sphenolithus radians*, 17: *Sphenolithus spiniger*, 18: *Braarudosphaera insecta*, 19: *Chiasmolithus oamaruensis*, 20: *Coccolithus eopelagicus*, 21: *Cribrocentrum reticulatum*, 22: *Discoaster barbadiensis*, 23: *Discoaster saipanensis*, 24: *Dictyococcites bisectus*, 25: *Ericsonia formosa*, 26: *Isthmolithus recurvus*, 27: *Pontosphaera obliquipons*, 28: *Pontosphaera ocellata*, 29: *Reticulofenestra dictyoda*, 30: *Reticulofenestra hillae*, 31: *Reticulofenestra umbilicus*..... 49

**Plate 5.2** Micrographs of calcareous nannofossil species found in samples D20 (1 - 17) and D24 (18 - 25). All scale bars on bottom right of each photograph represent length of 5μm. 1-3: *Cyclicargolithus abisectus*, 4-5: *Ericsonia formosa*, 6-8: *Helicosphaera recta*, 9: *Micula staurophora*, 10: *Pontosphaera punctosa*, 11-12: *Sphenolithus akropodus*, 13-14: *Sphenolithus distentus* ?, 15-17: *Sphenolithus predistentus*, 18: *Cyclicargolithus abisectus*, 19: *Discoaster barbadiensis*, 20: *Ericsonia formosa*, 21: *Isthmolithus recurvus*, 22-23: *Reticulofenestra hillae*, 24-25: *Sphenolithus tawfikii*. .... 54

**Plate 5.3** Micrographs of calcareous nannofossil species found in sample D28B (1-8), D28a (9-12), D27 (13-16), D17B (17-23). All scale bars on bottom right of each photograph represent length of 5μm. 1: *Chiasmolithus oamaruensis*, 2: *Cyclicargolithus abisectus*, 3: *Cribrocentrum reticulatum*, 4-6: *Sphenolithus predistentus*, 7: *Sphenolithus distentus*, 8: *Sphenolithus tawfikii*, 9: *Sphenolithus distentus*, 10: *Sphenolithus tawfikii*, 11: *Ericsonia formosa*, 12: *Sphenolithus predistentus*, 13: *Sphenolithus tawfikii*, 14: *Cribrocentrum reticulatum*, 15: *Discoaster barbadiensis*, 16: *Sphenolithus distentus*, 17: *Braarudosphaera bigelowii*, 18: *Cyclicargolithus abisectus*, 19-20: *Sphenolithus distentus*, 21-23: *Sphenolithus predistentus*. .... 59



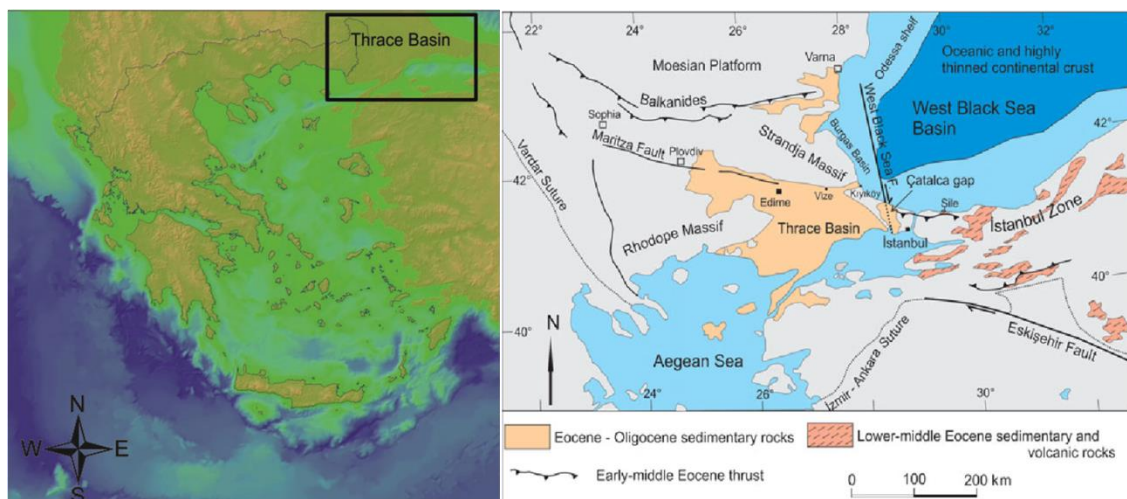


**Plate 5.4** Micrographs of calcareous nannofossil species found in samples D18 (1-9), D19 (10-19) and D29 (20-29). All scale bars on bottom right of each photograph represent length of 5 $\mu$ m. 1-3: *Cyclicargolithus abisectus*, 4: *Sphenolithus ciperoensis*, 5-7: *Sphenolithus distentus*, 8-9: *Sphenolithus predistentus*, 10: *Braarudosphaera perampla*, 11: *Sphenolithus ciperoensis*, 13-16: *Sphenolithus distentus*, 17-19: *Sphenolithus predistentus*, 20-21: *Cyclicargolithus abisectus*, 22-23: *Helicosphaera recta*, 24: *Micula staurophora*, 25: *Nannoconus kamptneri* subsp. *minor*, 26: *Sphenolithus ciperoensis*, 27-29: *Sphenolithus distentus*..... 67

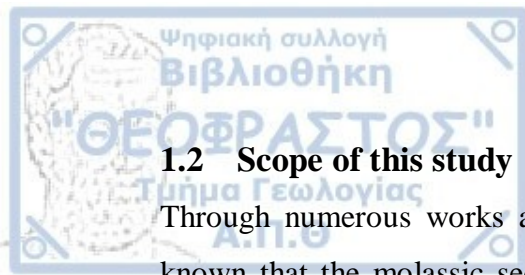
### 1.1 Study Area

The study area of this master thesis is the Western Thrace basin, located at the northeastern part of Greece.

In general, the Thrace basin is one of the largest Tertiary basins in the North Aegean region. It extends from NW Turkey (eastern Thrace basin) until NE Greece (western Thrace basin) including a small part in the SE Bulgaria. As shown by seismic sections and hydrocarbon wells (e.g., Kopp et al., 1969; Turgut et al., 1991; Görür & Okay, 1996) the Thrace basin hosts Eocene – Oligocene siliciclastic and Neogene – Quaternary sedimentary deposits of up to 9 km in thickness which are marginalized by the metamorphic rocks of Strandja and Rhodope massifs located in its northeastern and northwestern part, respectively.



**Figure 1.1 Left: The location of the Thrace basin in the NE Greece. Right: Map by Okay et al. (2019) showing the extent of its sedimentary rocks.**



## 1.2 Scope of this study

Through numerous works and the presence of nummulite bearing limestones it is known that the molassic sediments of the western Thrace basin show an age from Eocene to Oligocene (Christodoulou, 1958; Dragomanov et al., 1986; Roussos, 1994; Mainhold & BonDagher-Fadel, 2010).

Aim of this study is to analyze through polarized microscopy the nannofossil assemblages found in samples from the formations of Alexandroupolis sub-basin which is one of the three sub-basins that comprise the Western Thrace basin and also hosts the most complete sequence of the Tertiary formations. After this analysis the main objective is the biostratigraphical characterization of these samples by defining a biozone for each one using the biohorizons of identified index species and the biozonation schemes proposed by Martini 1971 and Agnini et al. 2014, eventually providing a more detailed dating of the molassic sediments of the Western Thrace basin.

## **2. Subject of this Study**

### **2.1 Calcareous Nannoplankton**

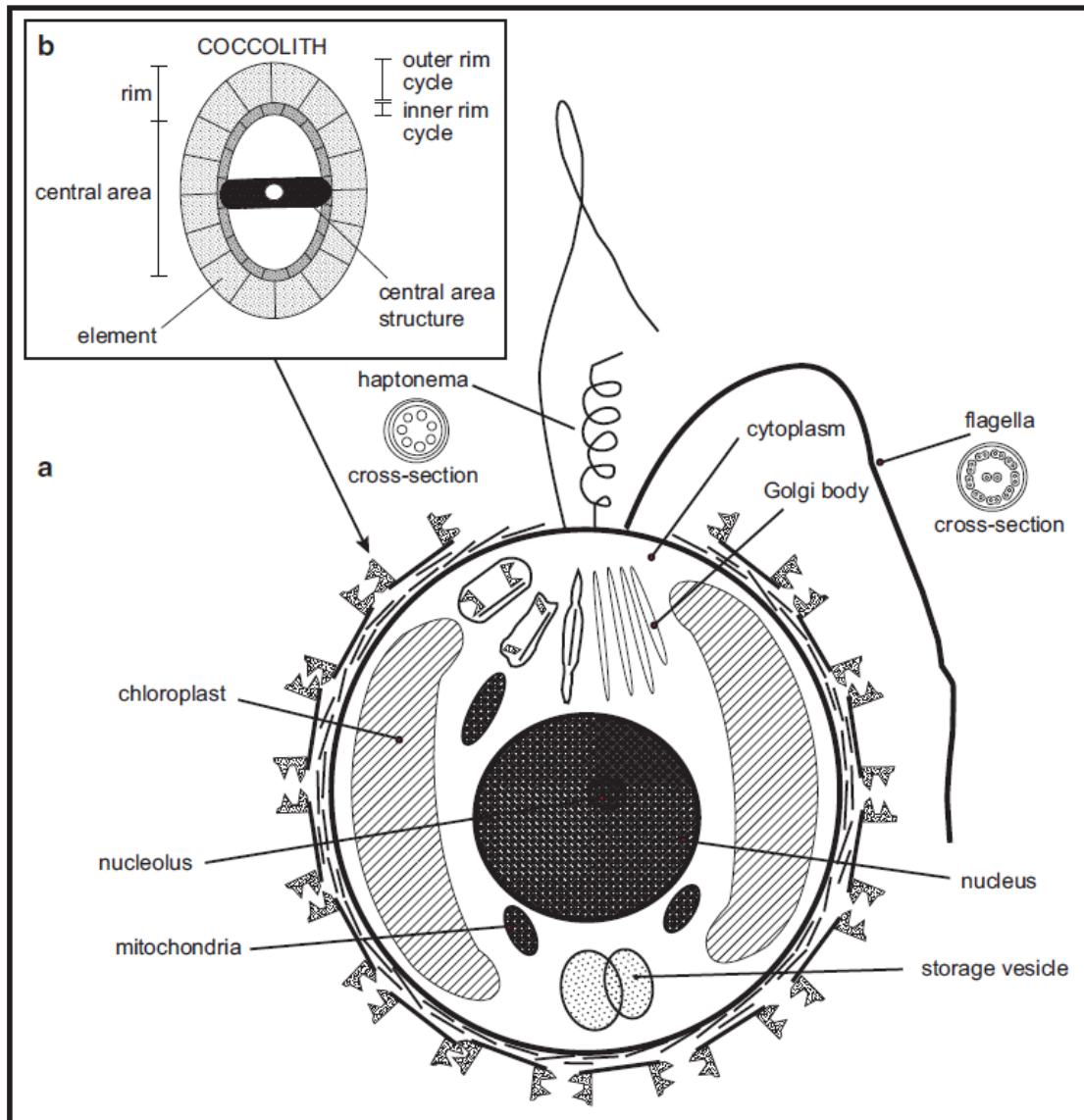
The term Calcareous nannoplankton or nannofossils is used to describe a heterogenous group of marine organisms and calcareous fossil structures. These organisms are smaller than 60  $\mu\text{m}$ , unicellular free floating marine phytoplankton and even though calcareous nannoplankton are largely diverse as a group, in the fossil state, the only representative that is found preserved are the coccoliths which are the calcitic plates that compose the coccolithophores.

Coccolithophores are the most dominant group of calcareous nannoplankton. They are marine unicellular autotrophic algae so their habitat is restricted to the photic zone, 0-200m depth of the water column. Taxonomically, they belong to Phylum Haptophyta and Division Prymnesiofyceae (Jordan & Chamberlain, 1997). Like most haptophytes, their eukaryotic cell possesses three flagella, two of the same length and one in a form of a coiled whip called “haptonema”. What differentiates them from the rest of this phylum is the ability to create numerous minute ( $<20\mu\text{m}$ ) coccoliths. Coccoliths are composed by calcium carbonate and a small amount of magnesium and by interlocking/overlapping each other, create a spherical exoskeleton that encloses the cell (coccosphere) (Figure 2.1.).

The life cycle of coccolithophores is characterized by “pleomorphism” which is the transition between a non motile diploid stage (2N) into one or more motile haploid stages (N). During these two stages the coccolithogenesis occurs which is the formation of two types of coccoliths;

- i. Heterococcoliths are formed during the diploid stage and are comprised of a radial array of complex shaped intergrown calcite crystals. They vary in form but they all share some basic morphological well distinct characteristics such as a radial structured rim and a central area which may be empty, crossed by bars, filled with a plate/net or bearing a spine.
- ii. Holococcoliths are formed during the haploid stage and are made of uniformly shaped minute calcite crystals held together by an organic matrix. In comparison to heterococcoliths, holococcoliths show great

homogeneity making difficult to distinct the rim from the central area and are less likely to be found preserved in fossil state.



**Figure 2.1** Schematic representation of (a) the structure and components of a coccolithophore cell and (b) the plan view of a single coccolith under microscope (Source: Bown & Young, 1998)

All the other forms of coccoliths that are different from the two types mentioned above consist a third informal group called “nannoliths”. Nannoliths are of similar size or larger than the other coccoliths and the shape of their structure varies considerably (starlike, rodshaped, florets, etc.).



## 2.2 The role of Calcareous Nannoplankton in the marine Carbon cycle

The marine Carbon cycle or Biological pump is the mechanism by which carbon-containing compounds are exported via biological processes from the surface to the deep ocean (Sarmiento & Gruber, 2004). Coccolithophores, which are considered to be the most productive calcifying organisms on earth, have a major role in the marine circulation of Carbon through two main processes; photosynthesis and calcification. (Figure 2.2)

Through photosynthesis ( $\text{CO}_2 + \text{H}_2\text{O} \rightarrow \text{CH}_2\text{O} + \text{O}_2$ ), coccolithophores accumulate carbon dioxide ( $\text{CO}_2$ ) in order to create organic matter while through the process of calcification ( $\text{HCO}_3^- + \text{Ca}^{2+} \rightarrow \text{CaCO}_3 + \text{H}_2\text{O}$ ) they produce carbon dioxide ( $\text{CO}_2$ ) in order to form coccoliths.

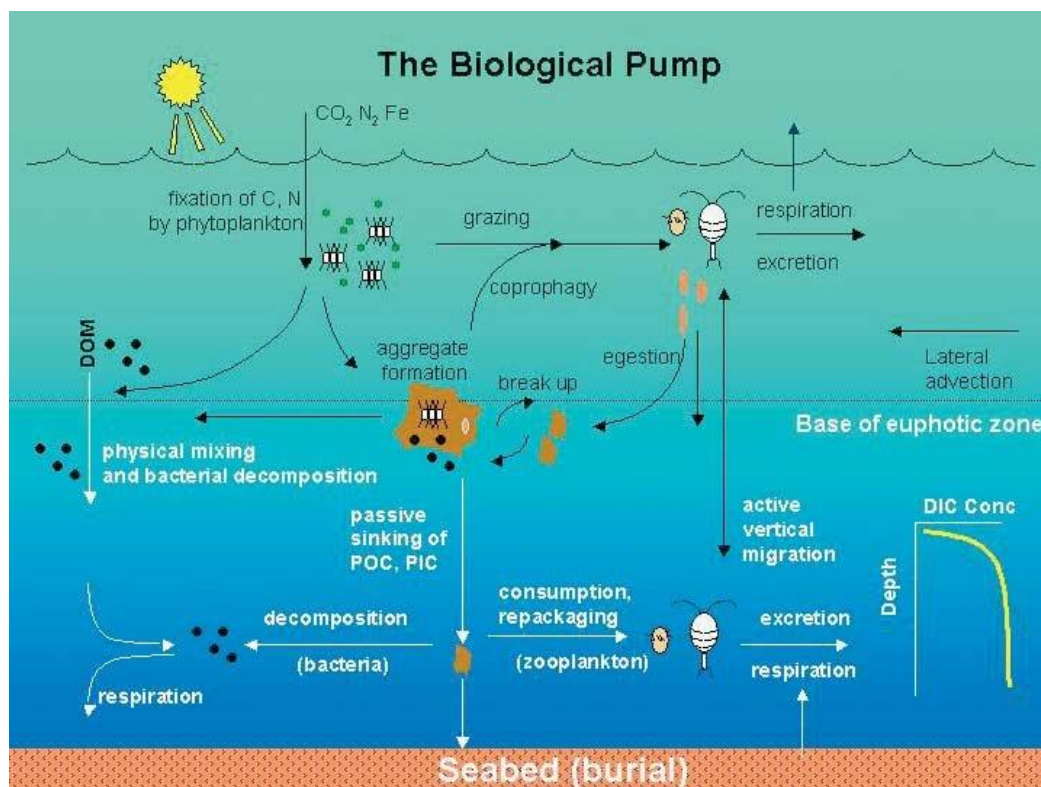
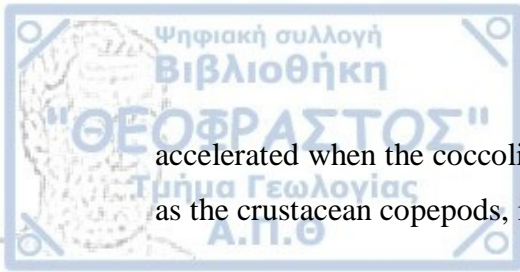


Figure 2.2 Schematic representation of the Biologic Pump (Ducklow, 2001)

Furthermore, coccolithophores contribute essentially (50%) in the total oceanic carbonate sediments (Milliman, 1993) as after their death their calcitic exoskeleton sinks through the water column until it reaches the sea floor above the carbonate compensation dept (CCD). This sinking is very slow as it is usual for the coccosphere to disintegrate into coccoliths after the death of the cell. This process though, gets



accelerated when the coccoliths are embedded in the fecal pellets of zooplankton such as the crustacean copepods, in that way they sink faster in the form of “marine snow”.

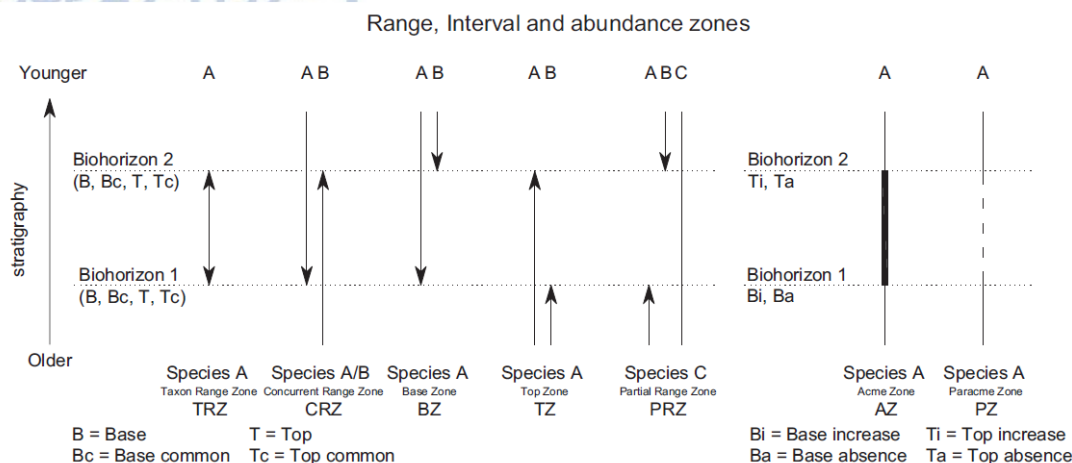
### **2.3 Calcareous Nannofossils as tools in Biostratigraphy**

Biostratigraphy is the branch of stratigraphy which through the use of fossils provides dating and correlation of rock formations and stratigraphic sequences in which they are discovered. The fundamental divisions of biostratigraphy are the biozones which are defined through the recognition of two or more biohorizons. A biohorizon can be described as the stratigraphic boundary where an alteration in the fossil content can be observed. The most basic biohorizons that are used in order to define a biozone are the first occurrences (Base, B), last occurrences (Top, T) of taxa as well as the beginning (Base common, Bc) and ending (Top common, Tc) of ranges when taxa start or stop being common and continuous.

These four types of biohorizons can define five different types of biozones (Agnini et al., 2017) (Figure 2.3):

- Species A Base Zone (BZ), defined as the interval between the Base of species A and the Base of species B.
- Species A Top Zone (TZ), defined as the interval between the Top of Species A and the Top of species B.
- Species A Taxon Range Zone (TRZ), defined as the interval between the Base and the Top of species A.
- Species A/species B Concurrent Range Biozone (CRZ), defined by the concurrent range of species A and species B.
- Species C Partial Range Zone (PRZ), comprised within the stratigraphical range of species C, between the Top of species A and the Base of species B.

Taxa whose biohorizons can provide valuable information and are used in defining of biozones are called index species.



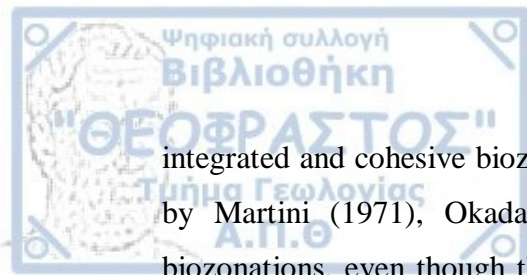
**Figure 2.3 Range, Interval and Abundance Zones used in calcareous nannofossil biozonations. (Redrawn by Agnini et al. 2017 after Wade et al., 2011 and Backman et al., 2012)**

Calcareous nannofossils provide undeniable qualities in biostratigraphic analysis making them an advantageous tool over other fossil groups, especially in industrial applications. First of all, calcareous nannofossils generally show very short stratigraphic ranges due to their rapid rate of evolution and disappearances of species. This characteristic, along with the fact that large amount of data was acquired during the Deep Ocean Drilling Programs since 1960, have advanced the resolution of nannofossil biostratigraphy by showing detailed first and last occurrences of species and thus creating new and more accurate biozones. The fact also that they derive from planktic organisms gives them the benefit of large biogeographic distribution which helps in the correlation of the same stratigraphical levels between wide areas.

Calcareous nannofossils are also abundant in marine carbonatic sediments which along with their miniscule size makes them very easy to collect as from just a small amount of sample millions of individuals can be gathered. Their size also provides them the advantage of being generally well preserved as mechanical damage is improbable. However, these characteristics come with some disadvantages as the preservation of nannofossils can get compromised in deep water sediments because of the dissolution of calcium carbonate below the carbonate compensation depth (CCD) while also their resistance to mechanical damage makes them susceptible to reworking.

The vast amount of data which has been gathered through decades concerning first and last occurrences of calcareous nannofossil taxa have led to the creation of





integrated and cohesive biozonations for the Cenozoic. The most notable are the ones by Martini (1971), Okada and Bukry (1980) and Bown et al. (1988). Those biozonations, even though they are generally accepted and still relevant today, have room for re-evaluation or further and more detailed division of zones, especially when it comes to regional alterations of the calcareous nannofossil record (e.g. differences between high and low latitudes). A great example, are two new biozonations for Neogene-Quaternary and Paleogene (Backman et al. 2012; Agnini et al. 2014), valid for middle-low latitudes, whose aim was to re-evaluate the ones by Martini (1971) and Okada & Bukry (1980) by validating or substituting, reliable or problematic biohorizons respectively.

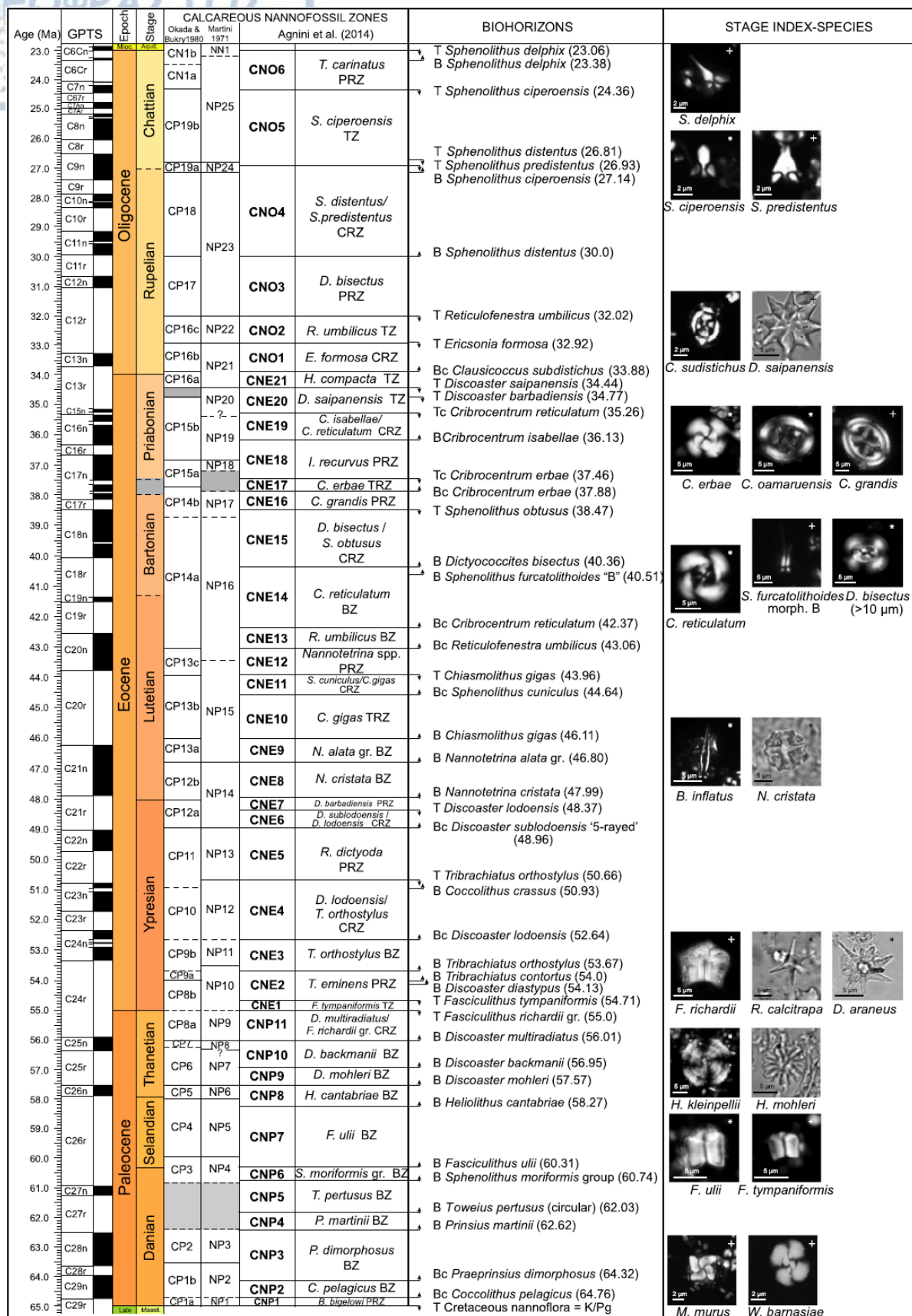
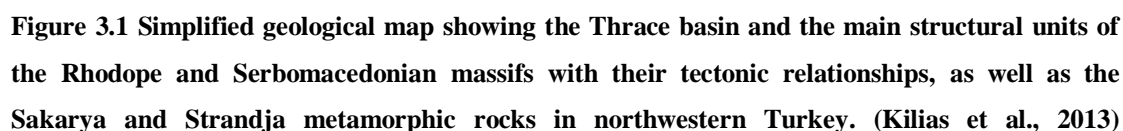
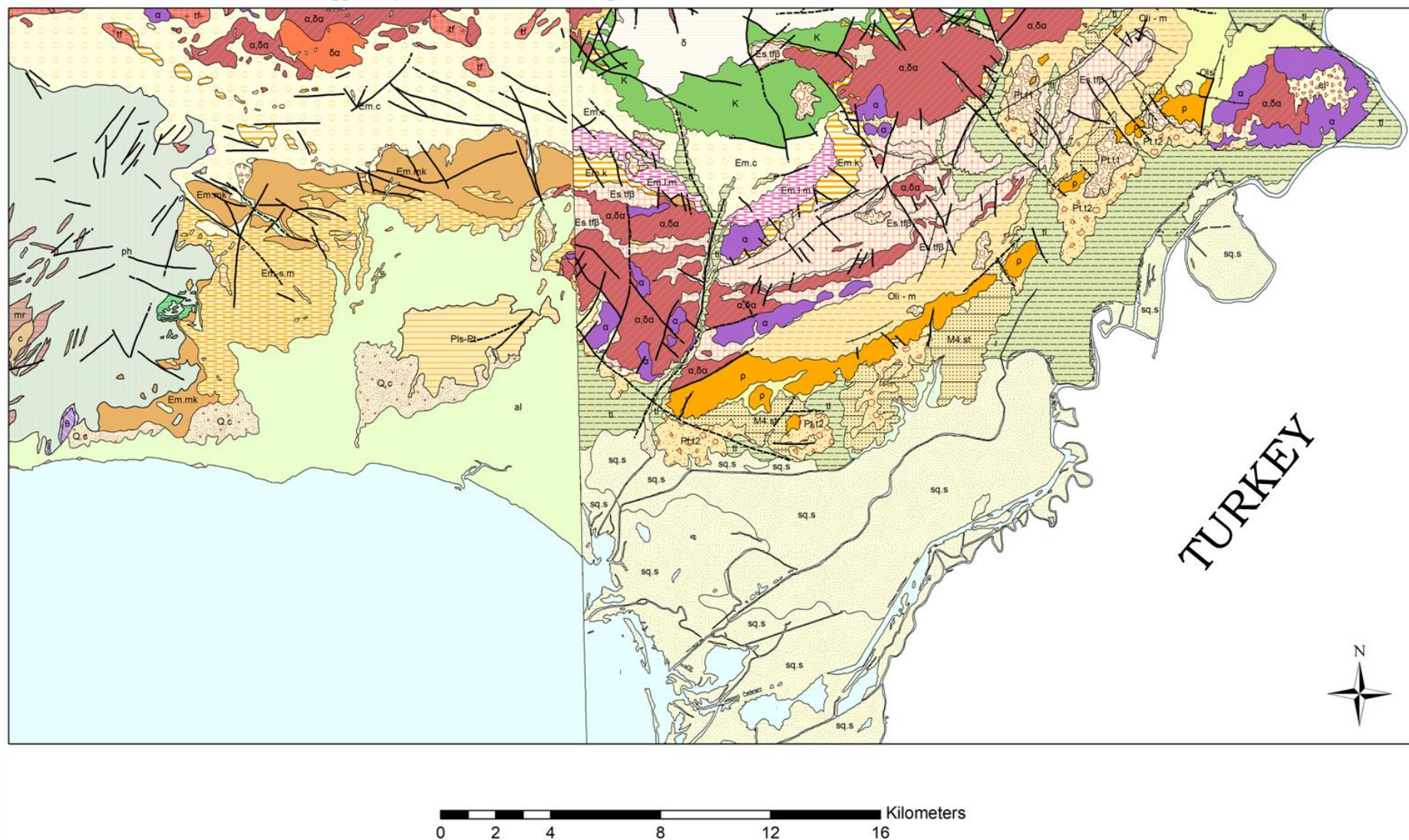


Figure 2.4 Palaeogene calcareous nannofossil biozonations. CP (Okada & Bukry 1980), NP (Martini, 1971), CN (Agnini et al., 2014). On the right, images of CN stage index-species are taken from literature. (\* = Base; + = Top; x = crossover) (Agnini et al., 2017)

















**Figure 3.2 Geological map of Alexandroupolis sheet (H.S.G.M.E., 1977) on the left and Ferai-Peplos-Ainos sheet (H.S.G.M.E., 1980) on the right.**

## Cenozoic

### Quaternary


-  Loam, sand, aggregate (al)
-  Recent torrential deposits (Q.c)
-  Lower stage of the lower terrace system (tl)
-  River mouth deposits (sq.s)
-  Scree (Q.sc)
-  Coastal deposits (cd)
-  Eluvial mantle (el)
-  Marine terrace (H.tm)

### Pleistocene (Terrestrial)

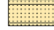
-  Lower terrace system (Pt.t2)
-  Upper terrace system (Pt.t1)

### Neogene

#### Upper Pliocene - Pleistocene

-  Gray clays (Pls - Pt)

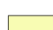

#### Upper Miocene

-  Marine Neogene of coastal facies (M4.st)


### Paleogene

#### Oligocene



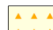

##### Chattian

-  Alternations of clays, marls and fine - grained sandstones with bioclastic banks (Lumachelle) (Ols)
-  Rhyolites (p)

##### Rupelian






-  Thin - bedded marls alternating with fine - platy sandstones, with intercalations of conglomerates and tuffs (Oli - m)

#### Molassic sediments of Eocene and Oligocene age




-  Marls and clays (Em - s.m)
-  Marls and clays (Em - s.mk)
-  Conglomeratic breccia (Em? br)
-  Middle Eocene (upper Lutetian) limestones (Em.mk)

#### Eocene


##### Priabonian


-  Sandy - calcareous facies of Nipsa (Es.tfa)
-  Sandy - marly, pyroclastic facies (Loutra Tavri)(Es.tfb)
-  Dacitoid andesites, dacites, rhyodacites (α,δα)
-  Dacite (δα)
-  Andesites (α)

##### Lower Priabonian - Upper Lutetian

-  Molassic type sediments (Em.k)
-  Clayey - marly series (Em.l.m)
-  Molassic type sediments (Em.c)

## Legend


-  Volcanic tuffs (tf)

-  The same volcanic tuffs(tf)

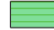

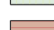
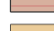



## Mesozoic and Older


### Cretaceous

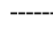
-  Diabase (δ)

-  Drimos - Melia series (K)

### Phyllitic system

-  Limestone (Js - Ki.k)
-  Phyllites argillaceous, sericitic and other schists and quartzites with weak or medium metamorphism (ph)
-  Marbles (mr)
-  Conglomerate, mainly of quartz pebbles (c)
-  Sandstones (st)
-  Gabbro - microgabbro, metamorphosed and schistosed (θ)
-  Amphibolitic - chloritic schists (sch.ab)

-  Fault

-  Fault probable or covered

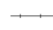
-  Fault with indications of displacement

Figure 3.3 Legend of figure 3.2 geological map.

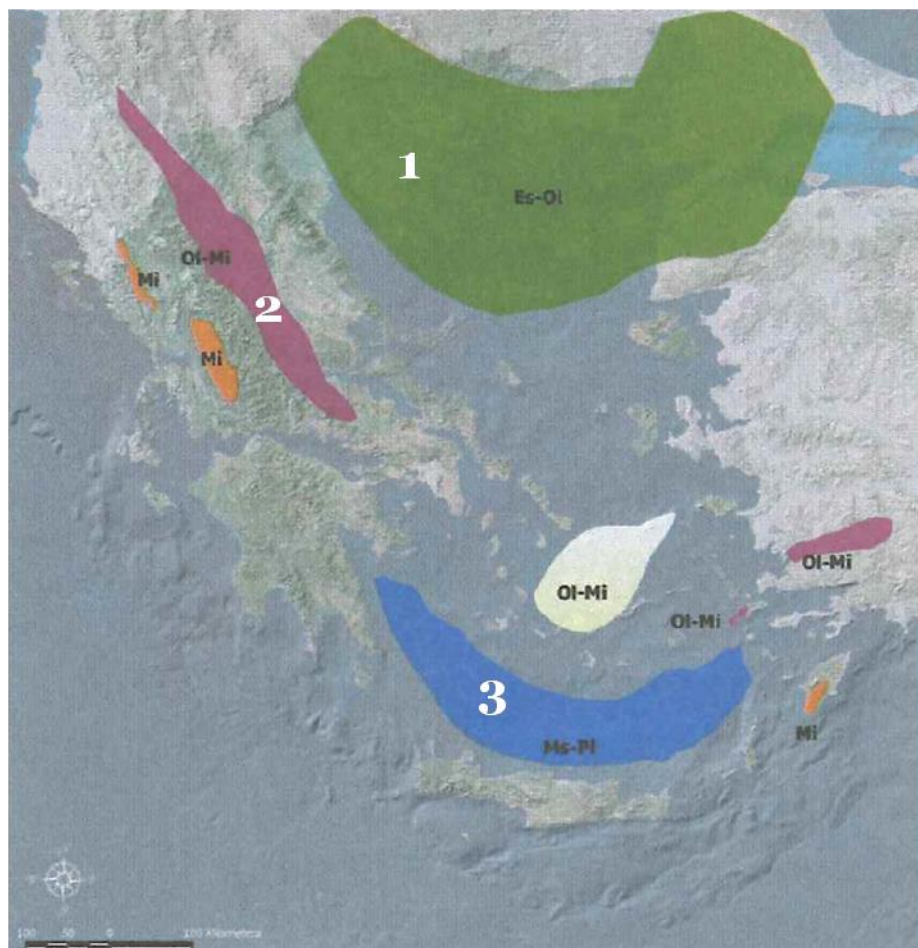


### 3.1 The Rhodope – North Aegean Molassic basin

The molassic formations of Greece can be grouped into three major molassic basins which have been developed in different locations and periods during the southward migration of the Hellenic arc (Παπανικολάου, 2015).

These molassic basins (Figure 3.4) are:

- The Rhodope – North Aegean molassic basin located at the core of the Hellenic arc and developed during Eocene – Oligocene.
- The Mesohellenic molassic Trough located at the middle of terrestrial Greece and developed during Oligocene – Middle Miocene.
- The Cretan Sea molassic basin, representing the back-arc basin of the Hellenic arc, still active since Upper Miocene.



**Figure 3.4 The major molassic basins of Greece. 1: Rhodope – North Aegean molassic basin, 2: Mesohellenic molassic Trough, 3: Cretan Sea molassic basin. (Παπανικολάου, 2015)**

The molassic formations that comprise the Western Thrace basin are part of the Rhodope – North Aegean molassic basin.

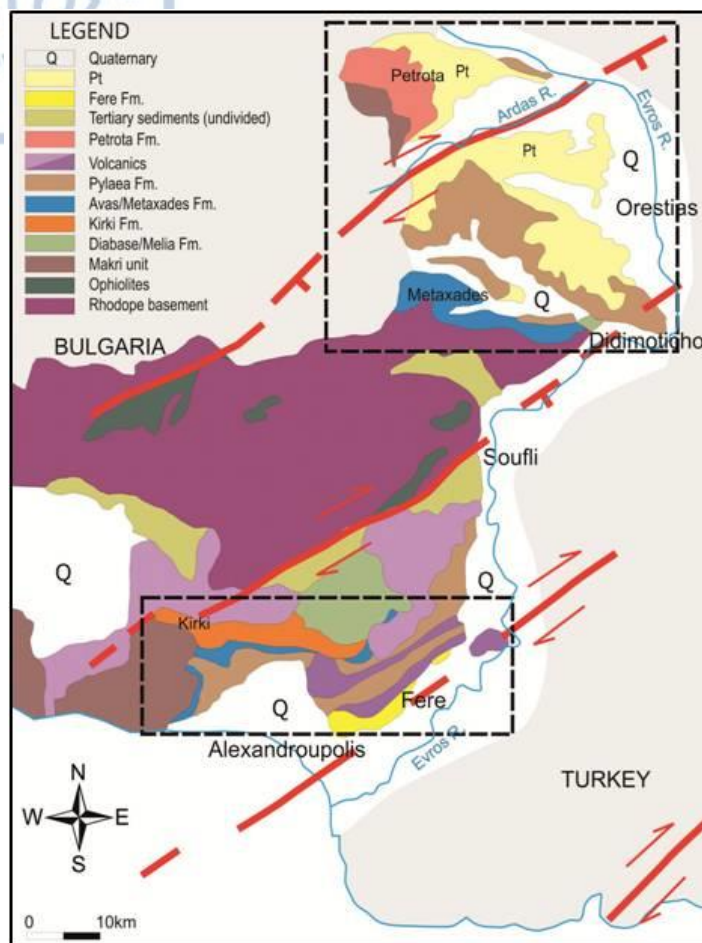
The Rhodope – North Aegean molasse has been deposited mainly on top of the metamorphic rocks of the Rhodope Massif as well as in the area of Vardar Zone (former Axios Zone). Its molassic formations also extent in the North Aegean Sea with the most notable observations on the islands of Limnos and Agios Efstratios.

In modern times there only a few appearances of the Rhodope – North Aegean molasse as its greatest part is either covered by the post-Alpine sediments of Upper Miocene – Pleistocene age or under the sea level in the North Aegean Sea or eroded.

The sedimentary rocks of the Molassic trough of Evros are conglomerates, sandstones, marles, argilaceous marles and marly limestones and their ages range from Low Eocene to the Oligocene/Miocene boundary (Kopp, 1966) while volcanism of mainly Oligocene age can also be observed.

### **3.2 Tectonostratigraphy of the Western Thrace basin**

Papanikolaou and Triantaphyllou (2010) have defined two NE-SW trending dextral strike-slip fault zones, the Soufli fault zone in the south and the Ardas fault zone in the north, dissecting the western part of Thrace Basin into three sub-basins (SB): the Petrota SB in the north, the Alexandroupolis SB in the south and the Orestias SB in the middle. (Figure 3.5)

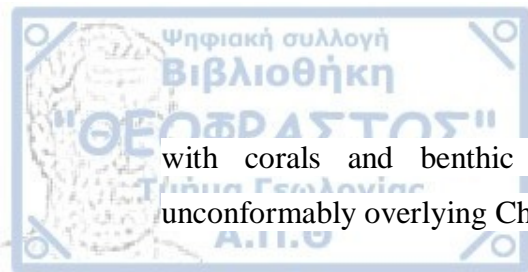


**Figure 3.5** The Western Thracian basin dissected by Ardas and Soufli fault zones into three sub-basins: Orestias SB, Petrota SB and Alexandroupolis SB. (Papanikolaou & Triantaphyllou, 2010)

The pre-Tertiary basement is different in the three western Thracian sub-basins. Medium-high grade metamorphic rocks are observed below the southern margin of Orestias SB and also below the western margin of Petrota SB. On the contrary, the low metamorphic grade Makri unit (part of the circum-Rhodope Unit) is observed below the western margin of Alexandroupolis SB, whereas the Melia Late Cretaceous alkaline volcanic activity (diabase and gabbro) and strongly folded and silicified “flysch”-type sediments are observed below the central part of the sub-Basin.

The Alexandroupolis SB consists of two Tertiary stratigraphic sequences separated by an angular unconformity. The lower sequence comprises the Kirki Formation, made of strongly folded and faulted sandstones, shales and reddish/greenish conglomerates, unconformably overlying the Melia “flysch”. Kirki Formation is overlain by a 30m thick sandstone member and by the Chorafaki Formation, made of alternations of sandstones and pelites. Avas Formation, comprising Eocene neritic reefal limestones





with corals and benthic foraminifera (e.g., Nummulites and Alveolina), is unconformably overlying Chorafaki Formation.

Upwards, the Pylaea Formation is made of tilted “flysh”-type marls, sandstones and some limestone interbeds. At the area around Fere, the Pylaea Formation contains thick volcanic rocks and pyroclastics. Towards the top, Pylaea Formation displays non deformed horizontal strata and the characteristic Pythion Member (near Didymoticho) with pronounced Congeria beds. The uppermost part of Pylaea is characterized by molassic-type cross-bedded sands, which are unconformably overlain by mostly lacustrine (?Miocene) deposits of Fere Formation.

The Orestias SB is featured only by the upper part of Alexandroupolis sequence, comprising Didymoticho and Pythion Formations Metaxades Formation, equivalent to Avas and Pylaea Formations of Alexandroupolis SB. Volcaniclastic sediments are located in the Metaxades area (e.g., Tsirambides et al, 1989). Towards the northwestern margin of Thrace Basin, a basal clastic formation of sandstones and conglomerates of Late Eocene age is exposed in the Petrota SB, overlain by marls of Oligocene age.

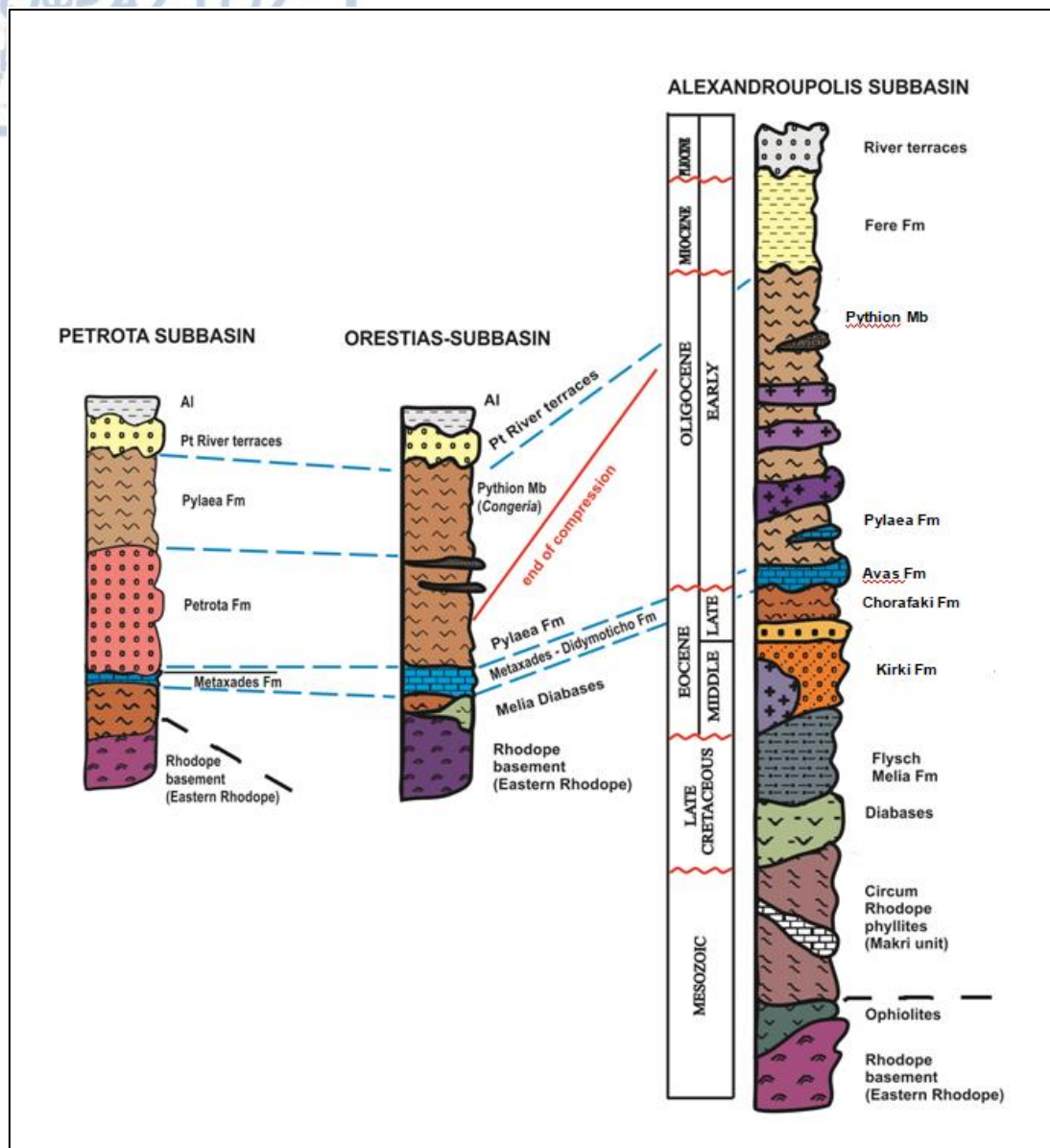


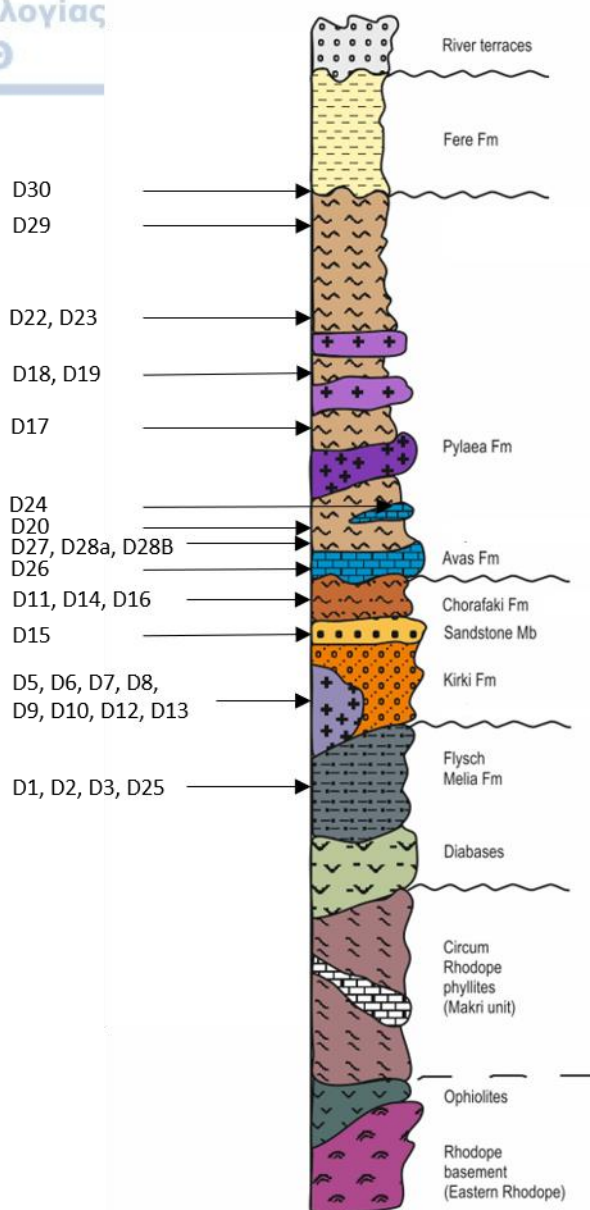
Figure 3.6 Correlated stratigraphic columns of the 3 sub-basins (Petrota SB, Orestias SB and Alexandroupolis SB) that comprise the Western Thrace basin. (Papanikolaou & Triantaphyllou, 2010)

## **4. Material and Methods**

### **4.1 Sampling**

In October of 2018 sampling was carried out on several outcrops, both natural and artificial, of the formations which comprise the Alexandroupolis sub-basin in the Western Thrace basin. In total, 44 samples were collected, by cleaning the outer layer of the outcrops and picking a small quantity of “healthy” sediment for each. During sampling, great attention was paid in avoiding contamination between samples and priority was given to the most clayey/argillaceous layers of the formations in order to maximize the possibility of richness and good preservation of nannofossils.

In order of stratigraphic succession the recovered samples were 4 from the Melia formation (D1, D2, D3, D25), 10 from Kirki Fm (D5, D6a, D6b, D7, D8, D9, D10, D12, D12-13A, D13), 1 from the sandstone member between Kirki Fm and Chorafaki Fm (D15), 11 from Chorafaki Fm (D11, D14, D16, D16A, D16B, D16Ca, D16Cb, D16D, D16E, D16Ea, D16F), 3 from Avas fm (D26, D26a, D26b) and 15 samples from Pylaea formation of which 1 was from the base (D20), 1 from the limestone lentil (D24), 11 from the middle (D28B, D28a, D27, D17, D17B, D18, D19, D21, D22, D23a, D23b) and 2 from the top (D29, D30) (Figure 4.1, Figure 4.2 and Figure 4.3).



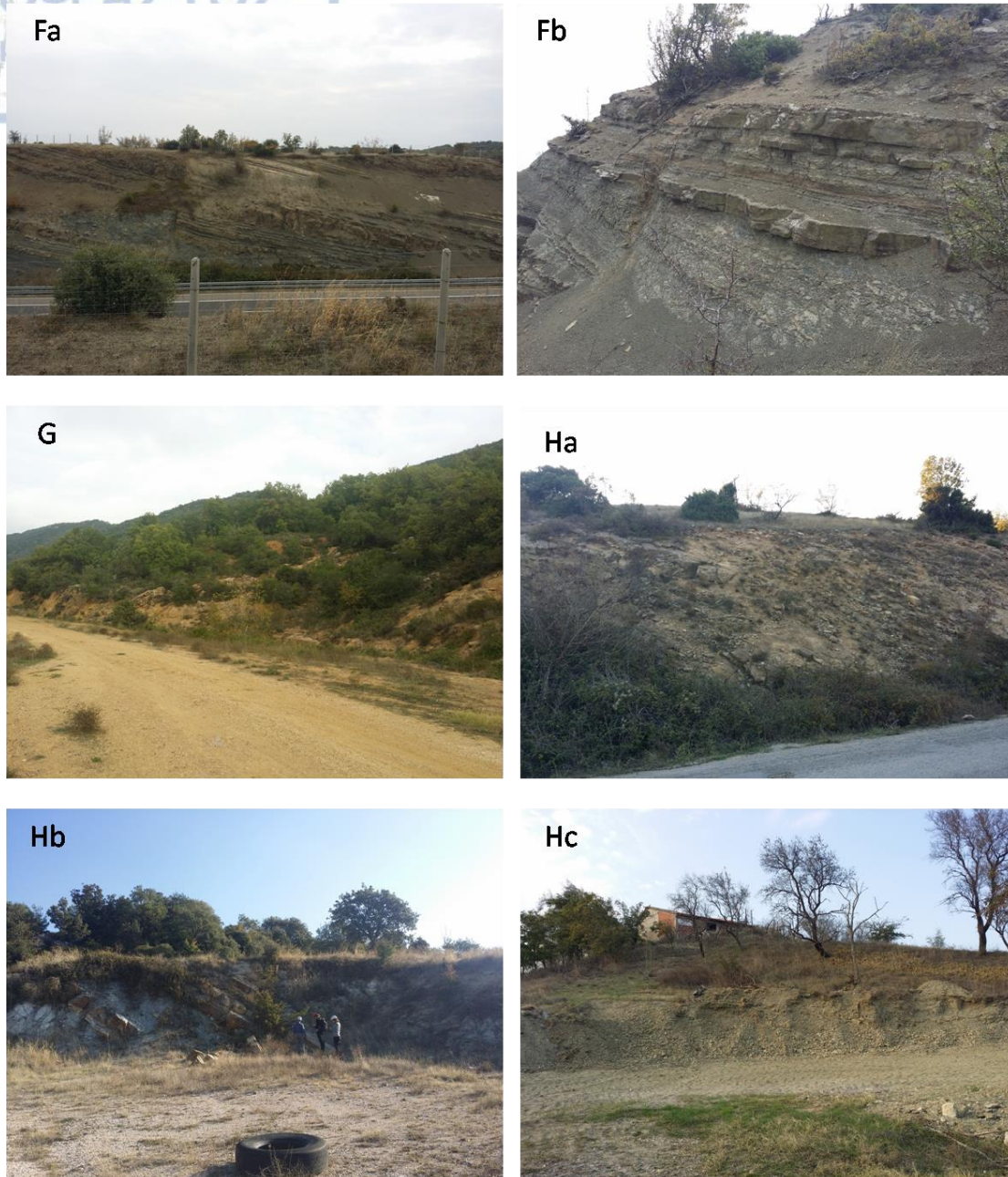
**Figure 4.1 Lithostratigraphic column of Alexandroupolis sub-basin and the collected samples.**  
(Papanikolaou & Triantaphyllou, 2010)





**Figure 4.2** Photos of outcrops showing the different formations and sampling points in the study area. A: Melia flysch (sample D1). B: Kirki formation (Ba. sample D6, Bb. sample D7). C: Kirki/Chorafaki (sample D15). D: Chorafaki formation (sample D16). E: Avas formation (sample D26)





**Figure 4.3** Photos of outcrops showing the different formations and sampling points in the study area. **F:** Lower Pylaea formation (Fa: sample D28, Fb: sample D27). **G:** Limestone lentil (sample D24). **H:** middle/upper Pylaea formation (Ha: sample D17B, Hb: samples D17/D18/D19, Hc: sample D29).

## 4.2 Calcareous nannofossil analysis

For the calcareous nannofossil analysis 51 smear slides were created, 1 slide for each sample while in some cases, due to color or lithological alterations in the same sample, the creation of a second one was deemed necessary (Table 4.1).

Table 4.1 List of all collected samples and smear slides which were analyzed

Code	Formation	Smear slides
D1	Melia Fm	1
D2		2
D3		1
D25		1
D5	Kirki Fm	1
D6a		2
D6b		1
D7		2
D8		1
D9		1
D10		1
D12		1
D12-13A		2
D13	1	
D15	Sandstone Mb	1
D11	Chorafaki Fm	1
D14		1
D16		1
D16A		2
D16B		1
D16Ca		1
D16Cb		1
D16D		1
D16E		1
D16Ea		1
D16F		1
D26	Avas Fm	1
D26a		1
D26b		1
D20	Pylaea Fm	1
D24		1
D28B		1
D28a		1
D27		1
D17		1
D17B		1
D18		1
D19		1
D21		1
D22		1
D23a		2
D23b		1
D29		1
D30		2
Total number of slides		51

#### 4.2.1 Sample preparation

The smear slides for calcareous nannofossil analysis have been prepared according to the standard preparation technique of Perch-Nielsen (1985). The steps of this preparation technique are mentioned below and are shown in Figure 4.4.

At first the sediment sample was cleaned by paring its outer surfaces (i). Then approximately 1-2 mm<sup>3</sup> of fine “dust” of material was scraped off with the use of a small metal tool and placed on a glass microscope slide (ii, iii). A drop of distilled water was then used to moisturize the material (iv) and a flat wooden toothpick to carefully smear it and create transverse lines across the slide (v, vi). Once these traverses were achieved the slide was placed on a VWR scientific hot plate until it dried out (vii). Afterwards, the side of the slide bearing the material was glued to a coverslip using a Norland optical adhesive 61 while applying slight pressure on it in order to avoid capturing air bubbles (viii, ix). Lastly, the slides were cleaned, labeled and were ready to be analyzed (x).



**Figure 4.4 Methodology of smear slide preparation for nannofossil analysis under polarized light microscope.**



#### 4.2.2 Analysis of samples

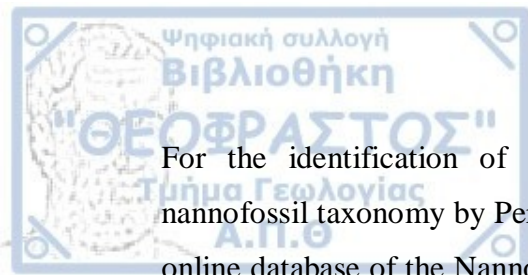
The smear slides were analyzed under a Leica DMLSP polarizing light microscope at 1250x. The majority of the samples collected were barren of nannofossils while the ones in which the nannofossils were present were intensely reworked and the state of preservation was mostly low, therefore, in order to accurately determine the biostratigraphic ranges, when needed, more than one smear slides for each sample were created and studied.



**Figure 4.5 Analysis of smear slides under polarized light microscope**

At first a semi-quantitative analysis has been followed, counting and identifying all species that were found in 3 traverses (1 traverse  $\approx$  100 fields of view) spanned across the slide, to determine which were common (C; 1 specimen/10 fields of view), rare (R; 1 specimen/10-100 fields of view), present (P; 1 specimen/ $>$ 100 fields of view) or reworked (RW). Due to the extreme rarity of index species and the inability of determining an exact biozone, the rest of each slide has also been studied counting and identifying any additional species especially index ones in order to conclude in a specific age. During this stage of the analysis, as index species were considered all taxa whose biohorizons are used in the division of biozones for the Paleogene period in general. Later on, once the data of all samples was collected and their relative age was possible to be determined, some of the index species, despite their presence, were disregarded as reworked.

In this study, the biostratigraphic indices *Sphenolithus predistentus*, *S. distentus* and *S. ciperoensis* are extremely rare in the assemblages and therefore considered to be in situ and not reworked as according to Backman and Shackleton (1983) when a species is rare it provides a poor source for reworking.



For the identification of all the different species, the detailed references for nannofossil taxonomy by Perch-Nielsen (1985) and Bown (1998) were used while the online database of the Nannotax project ([www.mikrotax.org/Nannotax3](http://www.mikrotax.org/Nannotax3)) by Young et al. (2017) has also been advised.

The biozonation that was used was the one according to Martini (1971) but also according to Agnini et al. (2014) as the last one provided modern data and more detailed biozones for the Paleogene period. The biostratigraphical scheme by Martini (1971) uses the alphanumerical notation “NP” (Nannoplankton Paleogene) for the Paleogene with a total number of 25 zones while the one by Agnini et al. (2014) uses “CN” (Calcareous Nannofossils) followed by letters indicating the Epoch (P: Palaeocene, E: Eocene, O: Oligocene).

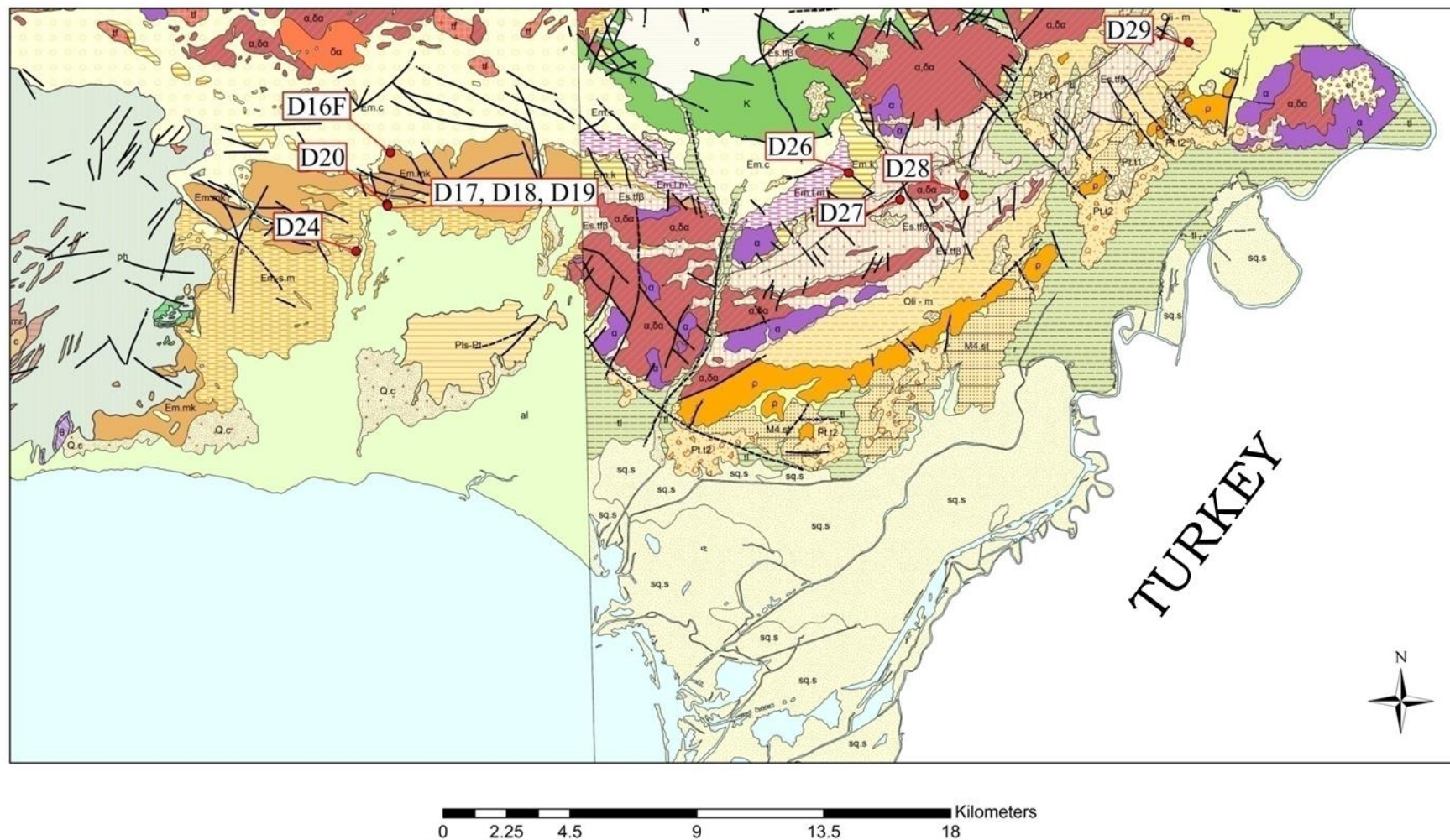


## 5. Results

Out of the 44 samples which were collected and studied, 33 were found to be barren of calcareous nannofossils. The 11 samples in which nannofossils were present (Figure 5.1 The outcrop positions from which the 11 samples that contained calcareous nannofossils were collected. Figure 5.1), in stratigraphic order from lower to higher, were:

- D16F from the base of Chorafaki Fm
- D26a from the base of Avas Fm
- D20 from the base of Pylaea Fm
- D24 from the limestone lentil in lower Pylaea Fm
- D28B, D28a, D27, D17B, D18 and D19 from the middle of Pylaea Fm
- D29 from the top of Pylaea Fm

As described in [Material and Methods](#) the analysis of each sample took place in two parts. At first all species found in 300 fields of view (FOV) were identified and counted while on the second part the whole smear slide ( $\approx 1500$  FOV) had to be studied counting only any additional species found, specifically index ones, thus concluding in a statistically safe result of the participation percentage of all species in each sample.





## 5.1 Chorafaki Formation

### Sample D16F

For sample D16F one smear slide has been studied under polarized light microscope. On Table 5.1 are shown the number of individual specimens of each species found in 3 traverses (300 FOV), randomly spanned across the smear slide. On Table 5.2, are shown the number of individual specimens of additional species found in the whole sample (1500 FOV). Finally, Figure 5.2 is a diagram showing the participation percentages of all species in the total nannofossil assemblage of sample D16F.

Table 5.1 Species and number of specimens found in 300 FOV in sample D16F.

D16F	
Species	Specimens / 300 FOV
<i>Blackites clavus</i>	4
<i>Campylosphaera dela</i>	3
<i>Chiasmolithus nitidus</i>	13
<i>Clausicoccus subdistichus</i>	4
<i>Coccolithus eopelagicus</i>	4
<i>Coccolithus pelagicus</i>	49
<i>Criboecentrum reticulatum</i>	10
<i>Cyclicargolithus floridanus</i>	38
<i>Dictyococcites bisectus</i>	15
<i>Ericsonia formosa</i>	19
<i>Reticulofenestra dictyoda</i>	4
<i>Reticulofenestra minuta</i>	11
<i>Sphenolithus furcatolithoides "morphotype A"</i>	10
<i>Sphenolithus furcatolithoides "morphotype B"</i>	21
<i>Sphenolithus moriformis</i>	25
<i>Sphenolithus radians</i>	1
<i>Sphenolithus spiniger</i>	24

Table 5.2 Additional species and number of specimens found in 1500 FOV in sample D16F.

D16F	
Species	Specimens / 1500 FOV
<i>Discoaster distinctus</i>	5
<i>Discoaster nodifer</i>	14
<i>Nannocomus funiculus</i>	1
<i>Neococcolithes dubius</i>	1
<i>Pontosphaera obliquipons</i>	4
<i>Reticulofenestra hillae</i>	15
<i>Reticulofenestra umbilicus</i>	7
<i>Sphenolithus conspicuus</i>	1
<i>Umbilicosphaera bramlettei</i>	2
<i>Zygrhablithus bijugatus</i>	6

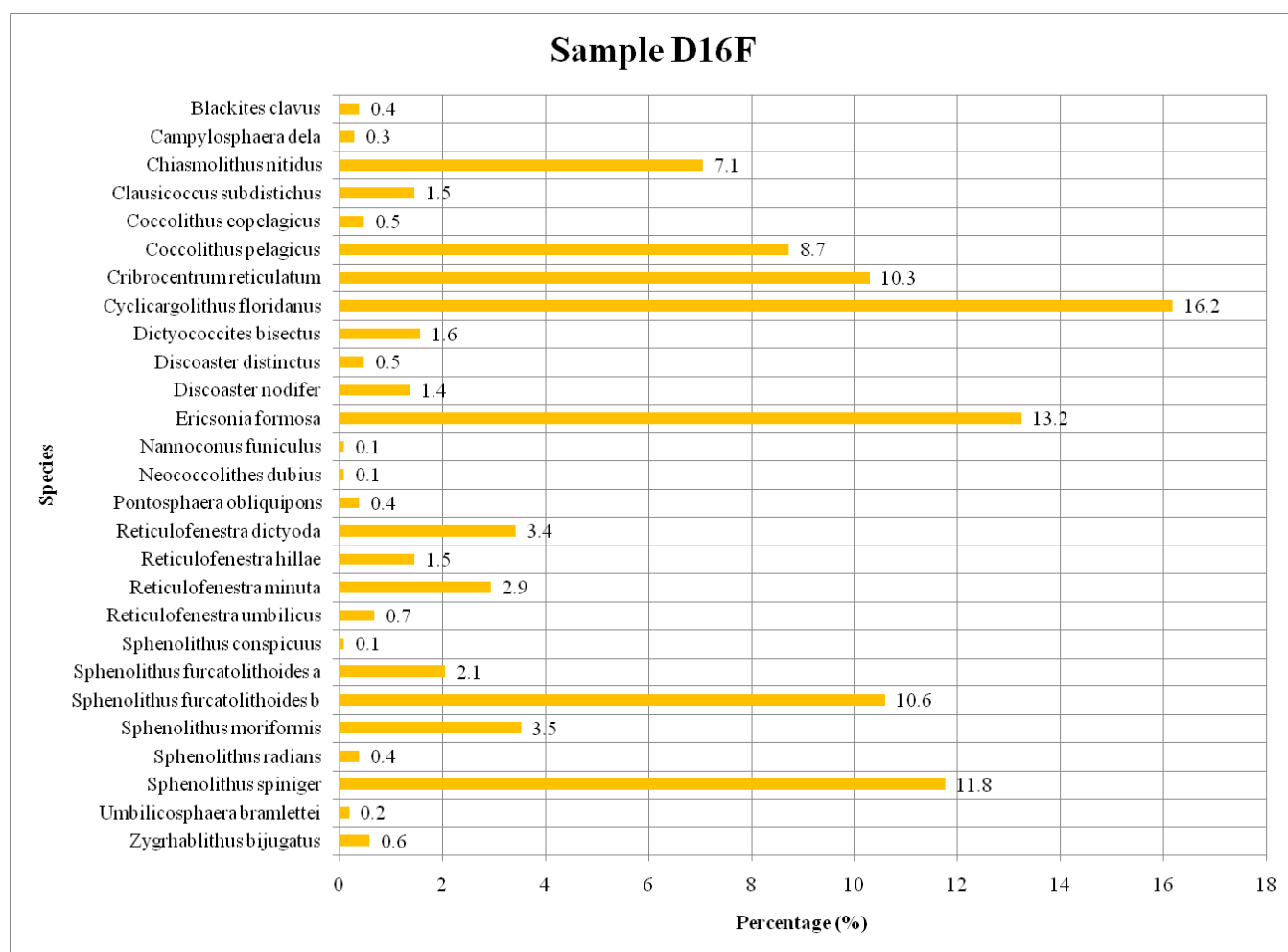


Figure 5.2 Participation percentages of nannofossil species in the whole smear slide of sample D16F.

## 5.2 Avas formation

### Sample D26a

For sample D26a one smear slide has been studied under polarized light microscope. On Table 5.3 are shown the number of individual specimens of each species found in 3 traverses (300 FOV), randomly spanned across the smear slide. On Table 5.4, are shown the number of individual specimens of additional species found in the whole sample (1500 FOV). Finally, Figure 5.3 is a diagram showing the participation percentages of all species in the total nannofossil assemblage of sample D26a.

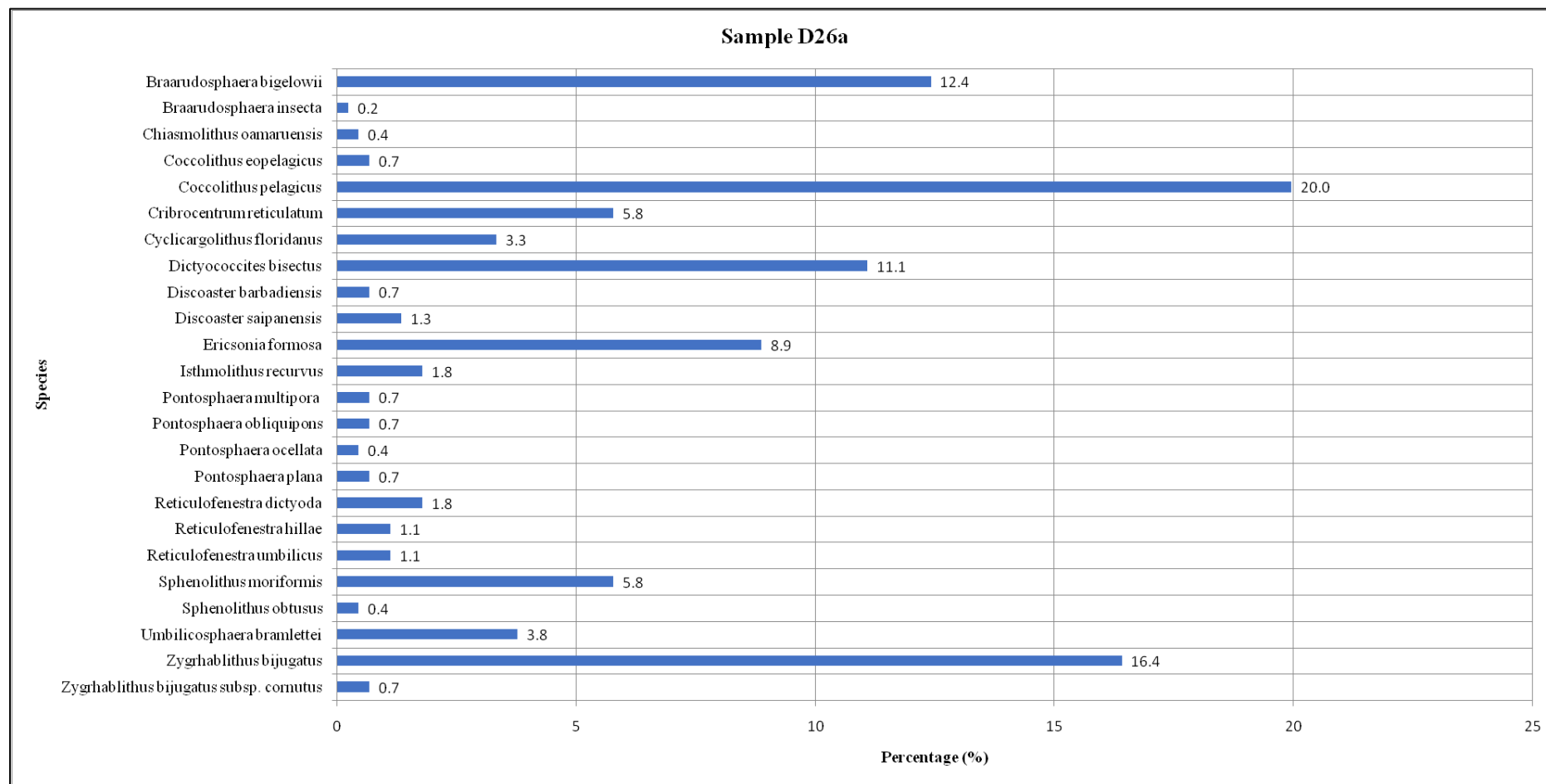
**Table 5.3 Species and number of specimens found in 300 FOV in sample D26a.**

D26a	
Species	Specimens / 300 FOV
<i>Braarudosphaera bigelowii</i>	11
<i>Coccolithus pelagicus</i>	18
<i>Cribrocentrum reticulatum</i>	5
<i>Cyclicargolithus floridanus</i>	3
<i>Dictyococcites bisectus</i>	10
<i>Discoaster saipanensis</i>	1
<i>Ericsonia formosa</i>	8
<i>Isthmolithus recurvus</i>	3
<i>Pontosphaera multipora</i>	1
<i>Pontosphaera obliquipons</i>	1
<i>Pontosphaera plana</i>	1
<i>Reticulofenestra dictyoda</i>	2
<i>Reticulofenestra hillae</i>	1
<i>Reticulofenestra umbilicus</i>	1
<i>Sphenolithus moriformis</i>	5
<i>Umbilicosphaera bramlettei</i>	3
<i>Zygrhablithus bijugatus</i>	15

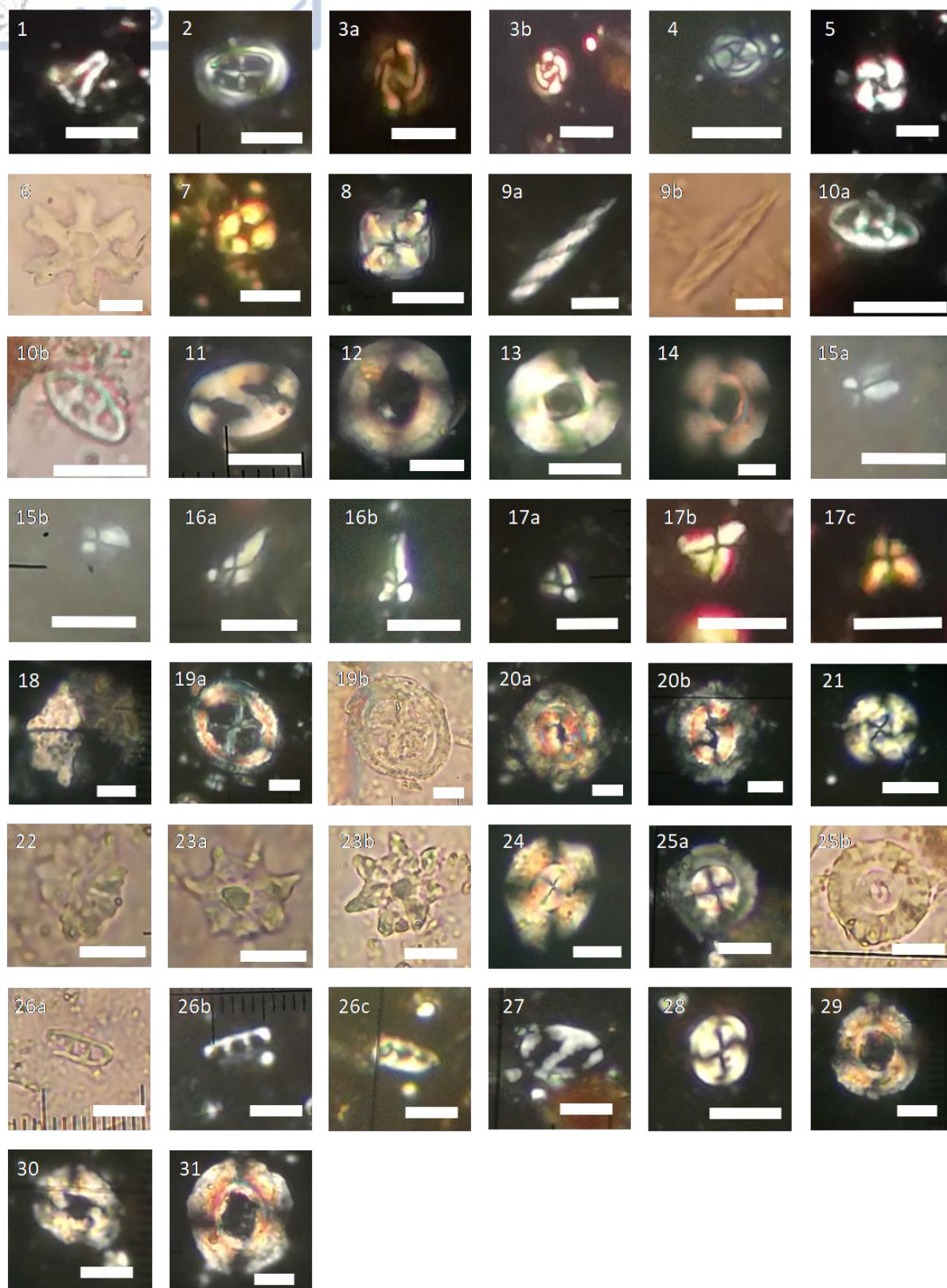
**Table 5.4 Additional species and number of specimens found in 1500 FOV in sample D26a.**

D26a	
Species	Specimens / 1500 FOV
<i>Braarudosphaera insecta</i>	1
<i>Chiasmolithus oamaruensis</i>	2
<i>Coccolithus eopelagicus</i>	3
<i>Discoaster barbadiensis</i>	3
<i>Pontosphaera ocellata</i>	2
<i>Sphenolithus obtusus</i>	2
<i>Zygrhablithus bijugatus subsp. cornutus</i>	3





**Figure 5.3 Participation percentages of nannofossil species in the whole smear slide of sample D26a.**



**Plate 5.1** Micrographs of calcareous nannofossil species found in samples D16F (1-17) and D26a (18-31). All scale bars on bottom right of each photograph represent length of 5μm. 1: *Blackites*

clavus, 2: *Campylosphaera dela*, 3: *Chiasmolithus nitidus*, 4: *Clausicoccus subdistichus*, 5: *Cribrocentrum reticulatum*, 6: *Discoaster distinctus*, 7: *Ericsonia formosa*, 8: *Micula staurophora*, 9: *Nannoconus funiculus*, 10: *Neococcolithes dubius*, 11: *Pontosphaera obliquipons*, 12: *Reticulofenestra dictyoda*, 13: *Reticulofenestra hillae*, 14: *Reticulofenestra umbilicus*, 15: *Sphenolithus furcatolithoides* "morphotype B", 16: *Sphenolithus radians*, 17: *Sphenolithus spiniger*, 18: *Braarudosphaera insecta*, 19: *Chiasmolithus oamaruensis*, 20: *Coccolithus eopelagicus*, 21: *Cribrocentrum reticulatum*, 22: *Discoaster barbadiensis*, 23: *Discoaster saipanensis*, 24: *Dictyococcites bisectus*, 25: *Ericsonia formosa*, 26: *Isthmolithus recurvus*, 27: *Pontosphaera obliquipons*, 28: *Pontosphaera ocellata*, 29: *Reticulofenestra dictyoda*, 30: *Reticulofenestra hillae*, 31: *Reticulofenestra umbilicus*.

### 5.3 Pylaea formation

#### Sample D20

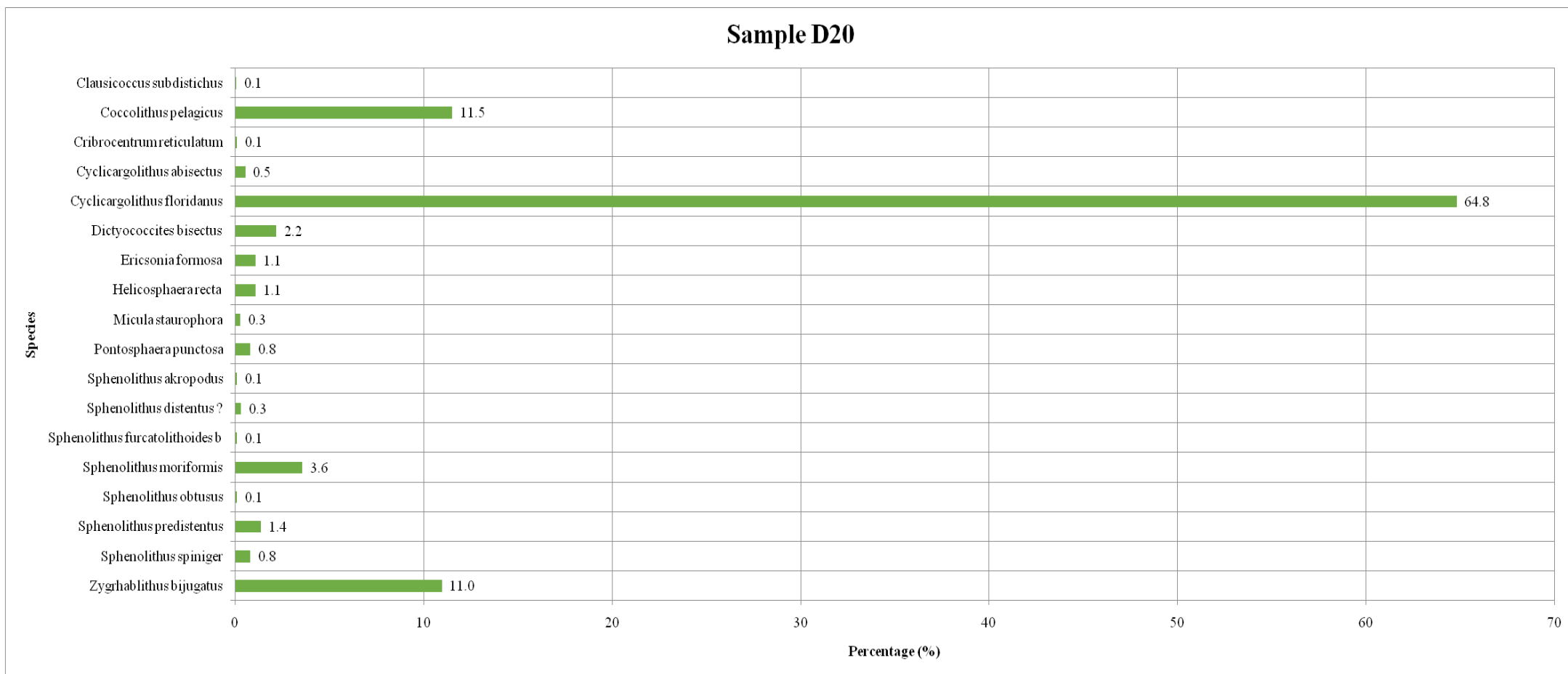
For sample D20 one smear slide has been studied under polarized light microscope. On Table 5.5 are shown the number of individual specimens of each species found in 3 traverses (300 FOV), randomly spanned across the smear slide. On Table 5.6, are shown the number of individual specimens of additional species found in the whole sample (1500 FOV). Finally, Figure 5.4 is a diagram showing the participation percentages of all species in the total nannofossil assemblage of sample D20.

Table 5.5 Species and number of specimens found in 300 FOV in sample D20.

D20	
Species	Specimens / 300 FOV
<i>Coccolithus pelagicus</i>	42
<i>Cyclicargolithus floridanus</i>	236
<i>Dictyococcites bisectus</i>	8
<i>Ericsonia formosa</i>	4
<i>Helicosphaera recta</i>	2
<i>Micula staurophora</i>	1
<i>Pontosphaera punctosa</i>	3
<i>Sphenolithus moriformis</i>	13
<i>Sphenolithus predistentus</i>	6
<i>Sphenolithus spiniger</i>	3
<i>Zygrhablithus bijugatus</i>	40

**Table 5.6 Additional species and number of specimens found in 1500 FOV in sample D20.**

D20	
Species	Specimens / 1500 FOV
<i>Clausicoccus subdistichus</i>	1
<i>Cribrocentrum reticulatum</i>	2
<i>Cyclicargolithus abisectus</i>	7
<i>Sphenolithus akropodus</i>	2
<i>Sphenolithus distentus</i> ?	6
<i>Sphenolithus furcatolithoides</i> "morphotype B"	2
<i>Sphenolithus obtusus</i>	2



**Figure 5.4 Participation percentages of nannofossil species in the whole smear slide of sample D20.**

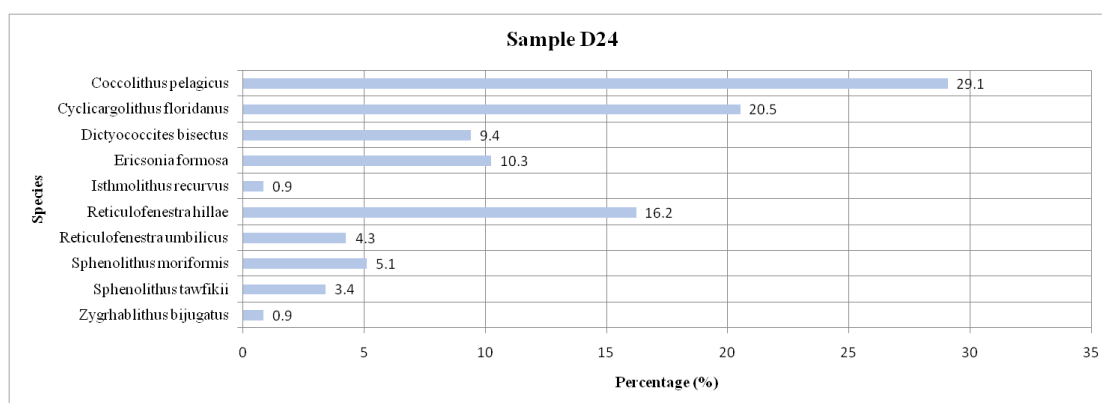


### Sample D24

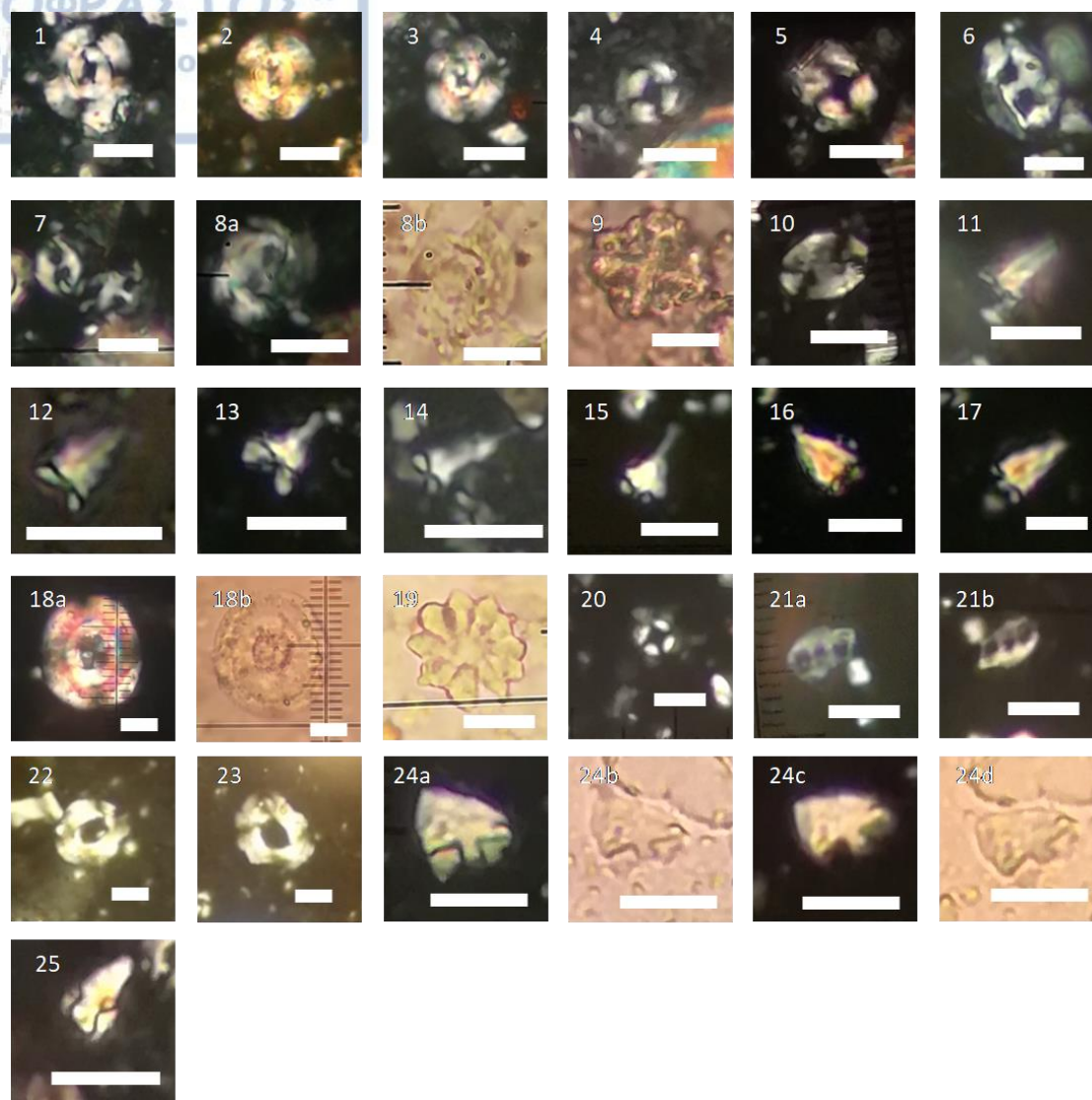
For sample D24 one smear slide has been studied under polarized light microscope. On Table 5.7 are shown the number of individual specimens of each species found in 3 traverses (300 FOV), randomly spanned across the smear slide. No additional species found in the rest of the sample. Finally, Figure 5.5 is a diagram showing the participation percentages of all species in the total nannofossil assemblage of sample D24.

**Table 5.7 Species and number of specimens found in 300 FOV in sample D24.**

D24	
Species	Specimens / 300 FOV
<i>Coccolithus pelagicus</i>	34
<i>Cyclicargolithus floridanus</i>	24
<i>Dictyococcites bisectus</i>	11
<i>Ericsonia formosa</i>	12
<i>Isthmolithus recurvus</i>	1
<i>Reticulofenestra hillae</i>	19
<i>Reticulofenestra umbilicus</i>	5
<i>Sphenolithus moriformis</i>	6
<i>Sphenolithus tawfikii</i>	4
<i>Zygrhablithus bijugatus</i>	1



**Figure 5.5 Participation percentages of nannofossil species in the whole smear slide of sample D24.**



**Plate 5.2** Micrographs of calcareous nannofossil species found in samples D20 (1 - 17) and D24 (18 - 25). All scale bars on bottom right of each photograph represent length of 5μm. 1-3: *Cyclicargolithus abisectus*, 4-5: *Ericsonia formosa*, 6-8: *Helicosphaera recta*, 9: *Micula staurophora*, 10: *Pontosphaera punctosa*, 11-12: *Sphenolithus akropodus*, 13-14: *Sphenolithus distentus* ?, 15-17: *Sphenolithus predistentus*, 18: *Cyclicargolithus abisectus*, 19: *Discoaster barbadiensis*, 20: *Ericsonia formosa*, 21: *Isthmolithus recurvus*, 22-23: *Reticulofenestra hillae*, 24-25: *Sphenolithus tawfikii*.

### **Sample D28B**

For sample D28B one smear slide has been studied under polarized light microscope. On Table 5.8 are shown the number of individual specimens of each species found in 3 traverses (300 FOV), randomly spanned across the smear slide. On Table 5.9, are shown the number of individual specimens of additional species found in the whole

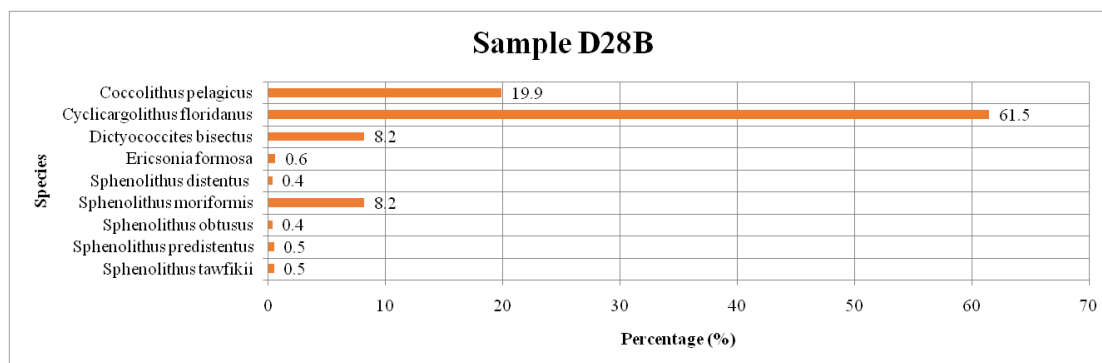
sample (1500 FOV). Finally, Figure 5.6 is a diagram showing the participation percentages of all species in the total nannofossil assemblage of sample D28B.

**Table 5.8 Species and number of specimens found in 300 FOV in sample D28B.**

D28B	
Species	Specimens / 300 FOV
<i>Coccolithus pelagicus</i>	34
<i>Cyclicargolithus floridanus</i>	105
<i>Dictyococcites bisectus</i>	14
<i>Ericsonia formosa</i>	1
<i>Sphenolithus moriformis</i>	14

**Table 5.9 Additional species and number of specimens found in 1500 FOV in sample D28B.**

D28B	
Species	Specimens / 1500 FOV
<i>Sphenolithus distentus</i>	3
<i>Sphenolithus obtusus</i>	3
<i>Sphenolithus predistentus</i>	4
<i>Sphenolithus tawfikii</i>	4



**Figure 5.6 Participation percentages of nannofossil species in the whole smear slide of sample D28B.**

### **Sample D28a**

For sample D28a one smear slide has been studied under polarized light microscope. On Table 5.10 are shown the number of individual specimens of each species found in 3 traverses (300 FOV), randomly spanned across the smear slide. On Table 5.11 are shown the number of individual specimens of additional species found in the whole

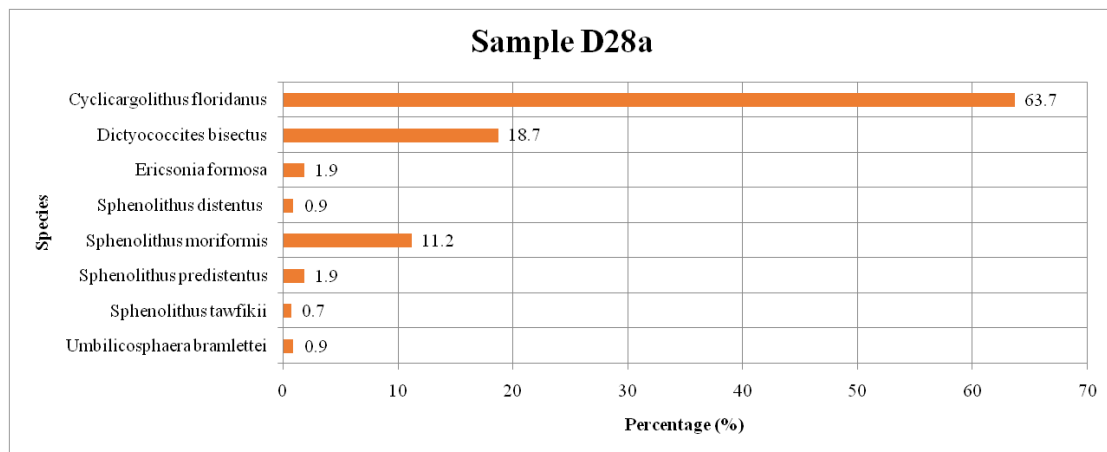
sample (1500 FOV). Finally, Figure 5.7 is a diagram showing the participation percentages of all species in the total nannofossil assemblage of sample D28a.

**Table 5.10 Species and number of specimens found in 300 FOV in sample D28a.**

D28a	
Species	Specimens / 300 FOV
<i>Cyclicargolithus floridanus</i>	68
<i>Dictyococcites bisectus</i>	20
<i>Ericsonia formosa</i>	2
<i>Sphenolithus moriformis</i>	12
<i>Sphenolithus predistentus</i>	2
<i>Umbilicosphaera bramlettei</i>	1

**Table 5.11 Additional species and number of specimens found in 1500 FOV in sample D28a.**

D28a	
Species	Specimens / 1500 FOV
<i>Sphenolithus distentus</i>	5
<i>Sphenolithus tawfikii</i>	4



**Figure 5.7 Participation percentages of nannofossil species in the whole smear slide of sample D28a.**

### **Sample D27**

For sample D27 one smear slide has been studied under polarized light microscope. On Table 5.12 are shown the number of individual specimens of each species found in 3 traverses (300 FOV), randomly spanned across the smear slide. On Table 5.13 are

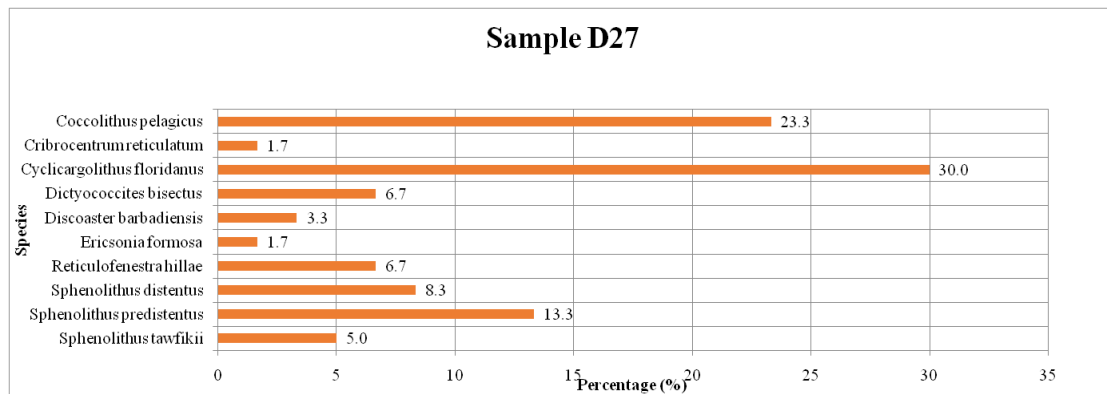
shown the number of individual specimens of additional species found in the whole sample (1500 FOV). Finally, Figure 5.8 is a diagram showing the participation percentages of all species in the total nannofossil assemblage of sample D27.

**Table 5.12 Species and number of specimens found in 300 FOV in sample D27.**

D27	
Species	Specimens / 300 FOV
<i>Coccolithus pelagicus</i>	14
<i>Cribocentrum reticulatum</i>	1
<i>Cyclicargolithus floridanus</i>	18
<i>Dictyococcites bisectus</i>	4
<i>Discoaster barbadiensis</i>	2
<i>Ericsonia formosa</i>	1
<i>Reticulofenestra hillae</i>	4

**Table 5.13 Additional species and number of specimens found in 1500 FOV in sample D27.**

D27	
Species	Specimens / 1500 FOV
<i>Sphenolithus distentus</i>	5
<i>Sphenolithus predistentus</i>	8
<i>Sphenolithus tawfikii</i>	3



**Figure 5.8 Participation percentages of nannofossil species in the whole smear slide of sample D27.**

### **Sample D17B**

For sample D17B one smear slide has been studied under polarized light microscope. On Table 5.14 are shown the number of individual specimens of each species found in



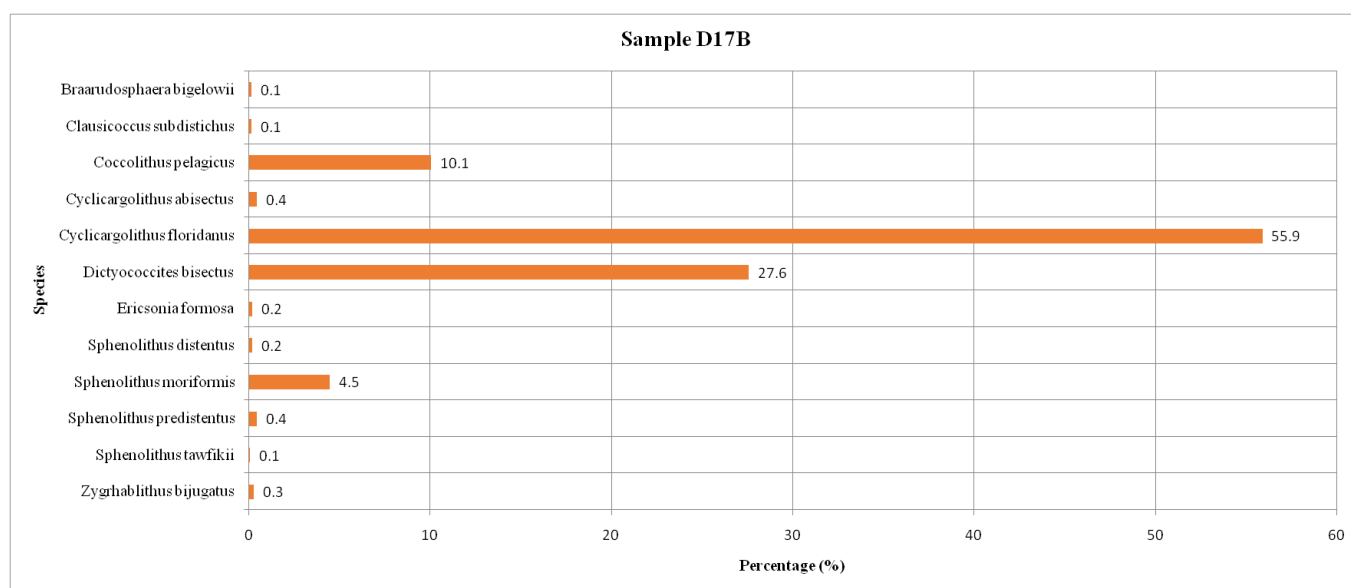
3 traverses (300 FOV), randomly spanned across the smear slide. On Table 5.15, are shown the number of individual specimens of additional species found in the whole sample (1500 FOV). Finally, Figure 5.9 is a diagram showing the participation percentages of all species in the total nannofossil assemblage of sample D17B.

**Table 5.14 Species and number of specimens found in 300 FOV in sample D17B.**

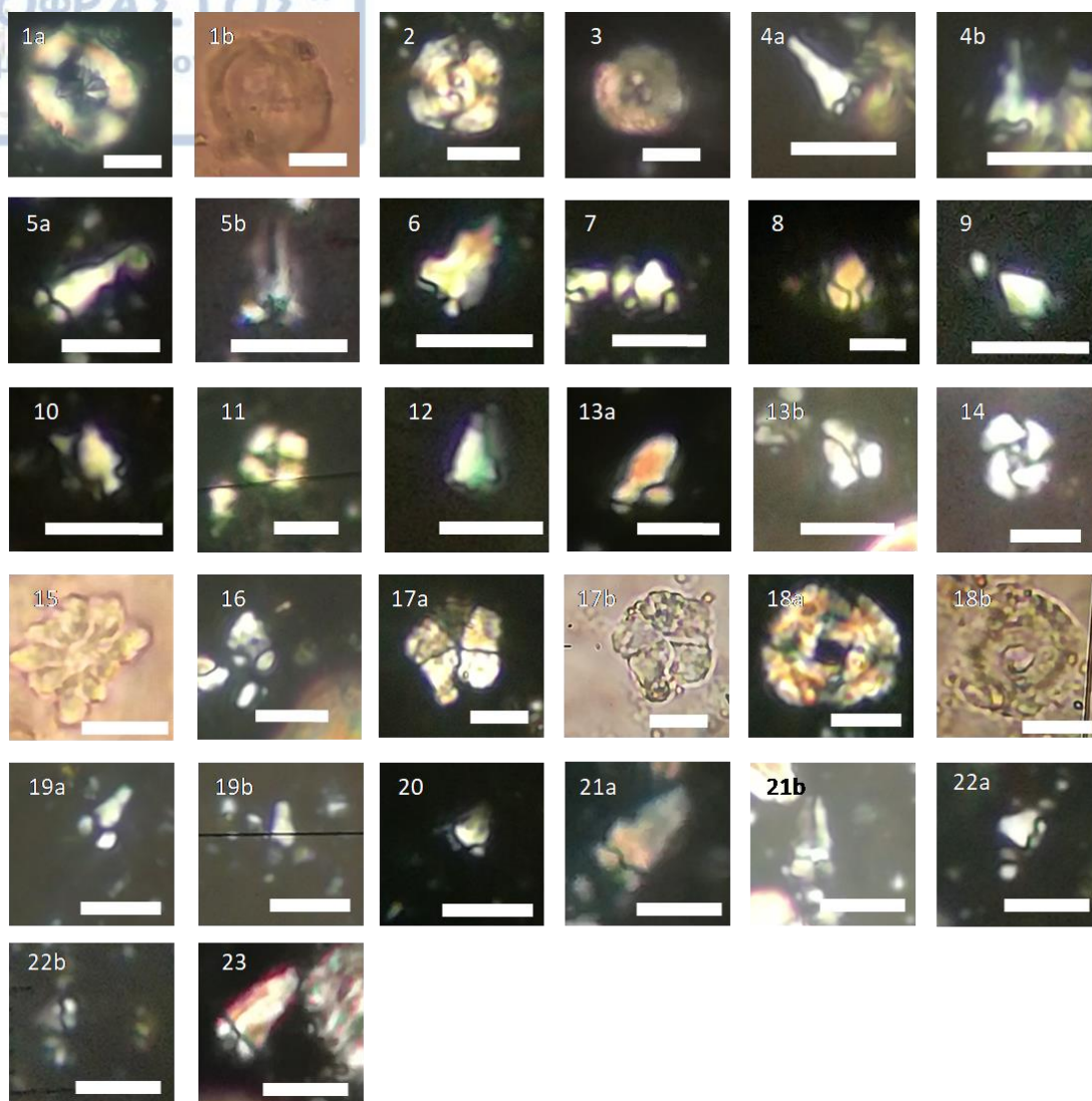
D17B	
Species	Specimens / 300 FOV
<i>Coccolithus pelagicus</i>	27
<i>Cyclicargolithus floridanus</i>	150
<i>Dictyococcites bisectus</i>	74
<i>Sphenolithus moriformis</i>	12

**Table 5.15 Additional species and number of specimens found in 1500 FOV in sample D17B.**

D17B	
Species	Specimens / 1500 FOV
<i>Braarudosphaera bigelowii</i>	2
<i>Clausicoccus subdistichus</i>	2
<i>Cyclicargolithus abisectus</i>	6
<i>Ericsonia formosa</i>	3
<i>Sphenolithus distentus</i>	3
<i>Sphenolithus predistentus</i>	6
<i>Sphenolithus tawfikii</i>	1
<i>Zygrhablithus bijugatus</i>	4



**Figure 5.9 Participation percentages of nannofossil species in the whole smear slide of sample D17B.**



**Plate 5.3** Micrographs of calcareous nannofossil species found in sample D28B (1-8), D28a (9-12), D27 (13-16), D17B (17-23). All scale bars on bottom right of each photograph represent length of 5μm. 1: *Chiasmolithus oamaruensis*, 2: *Cyclicargolithus abisectus*, 3: *Cribocentrum reticulatum*, 4-6: *Sphenolithus predistentus*, 7: *Sphenolithus distentus*, 8: *Sphenolithus tawfikii*, 9: *Sphenolithus distentus*, 10: *Sphenolithus tawfikii*, 11: *Ericsonia formosa*, 12: *Sphenolithus predistentus*, 13: *Sphenolithus tawfikii*, 14: *Cribocentrum reticulatum*, 15: *Discoaster barbadiensis*, 16: *Sphenolithus distentus*, 17: *Braarudosphaera bigelowii*, 18: *Cyclicargolithus abisectus*, 19-20: *Sphenolithus distentus*, 21-23: *Sphenolithus predistentus*.



### **Sample D18**

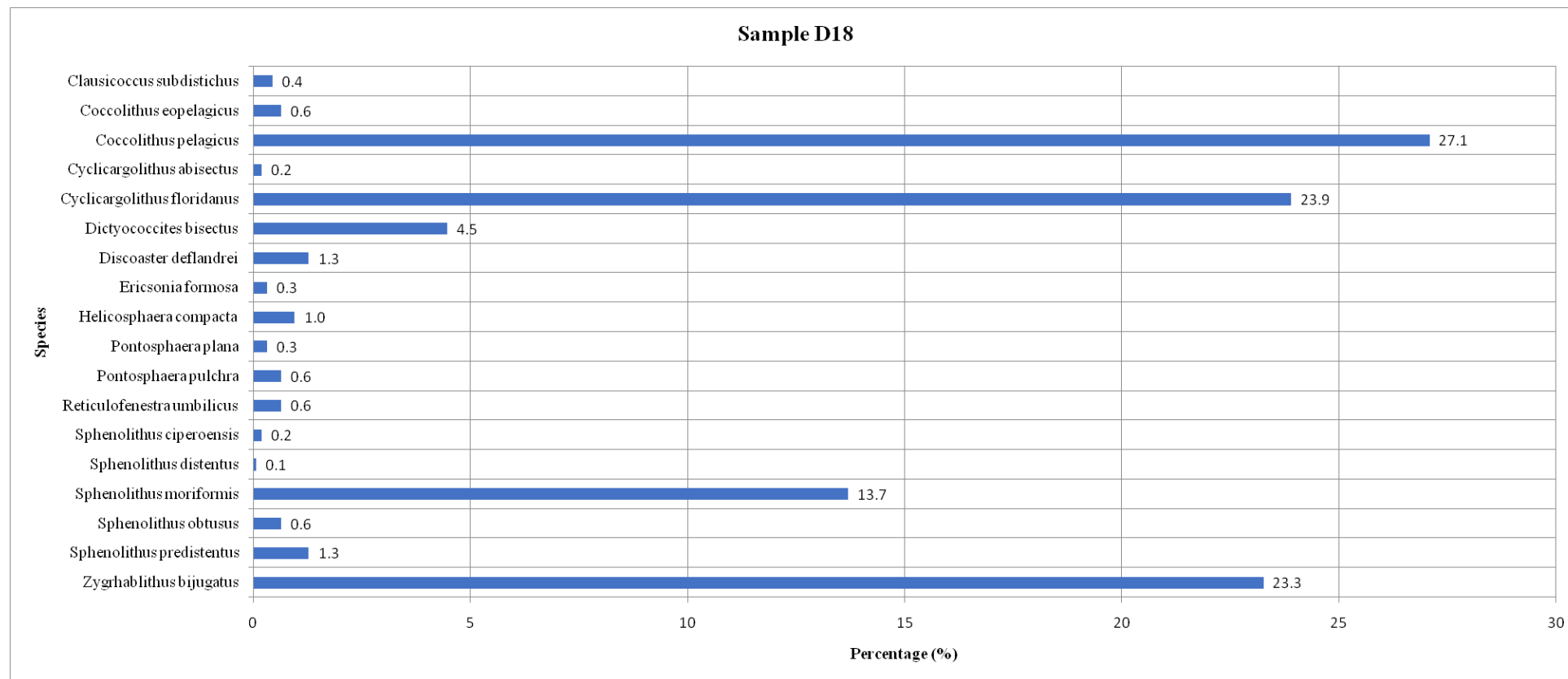
For sample D18 one smear slide has been studied under polarized light microscope. On Table 5.16 are shown the number of individual specimens of each species found in 3 traverses (300 FOV), randomly spanned across the smear slide. On Table 5.17, are shown the number of individual specimens of additional species found in the whole sample (1500 FOV). Finally, Figure 5.10 is a diagram showing the participation percentages of all species in the total nannofossil assemblage of sample D18.

**Table 5.16 Species and number of specimens found in 300 FOV in sample D18.**

<b>D18</b>	
<b>Species</b>	<b>Specimens / 300 FOV</b>
<i>Coccolithus eopelagicus</i>	2
<i>Coccolithus pelagicus</i>	85
<i>Cyclicargolithus floridanus</i>	75
<i>Dictyococcites bisectus</i>	14
<i>Discoaster deflandrei</i>	4
<i>Ericsonia formosa</i>	1
<i>Helicosphaera compacta</i>	3
<i>Pontosphaera plana</i>	1
<i>Pontosphaera pulchra</i>	2
<i>Reticulofenestra umbilicus</i>	2
<i>Sphenolithus moriformis</i>	43
<i>Sphenolithus obtusus</i>	2
<i>Sphenolithus predistentus</i>	4
<i>Zygrhablithus bijugatus</i>	73

**Table 5.17 Additional species and number of specimens found in 1500 FOV in sample D18.**

<b>D18</b>	
<b>Species</b>	<b>Specimens / 1500 FOV</b>
<i>Clausicoccus subdistichus</i>	7
<i>Cyclicargolithus abisectus</i>	3
<i>Sphenolithus ciperoensis</i>	3
<i>Sphenolithus distentus</i>	1



**Figure 5.10** Participation percentages of nannofossil species in the whole smear slide of sample D18.



### **Sample D19**

For sample D19 one smear slide has been studied under polarized light microscope. On Table 5.18 are shown the number of individual specimens of each species found in 3 traverses (300 FOV), randomly spanned across the smear slide. On Table 5.19, are shown the number of individual specimens of additional species found in the whole sample (1500 FOV). Finally, Figure 5.11 is a diagram showing the participation percentages of all species in the total nannofossil assemblage of sample D19.

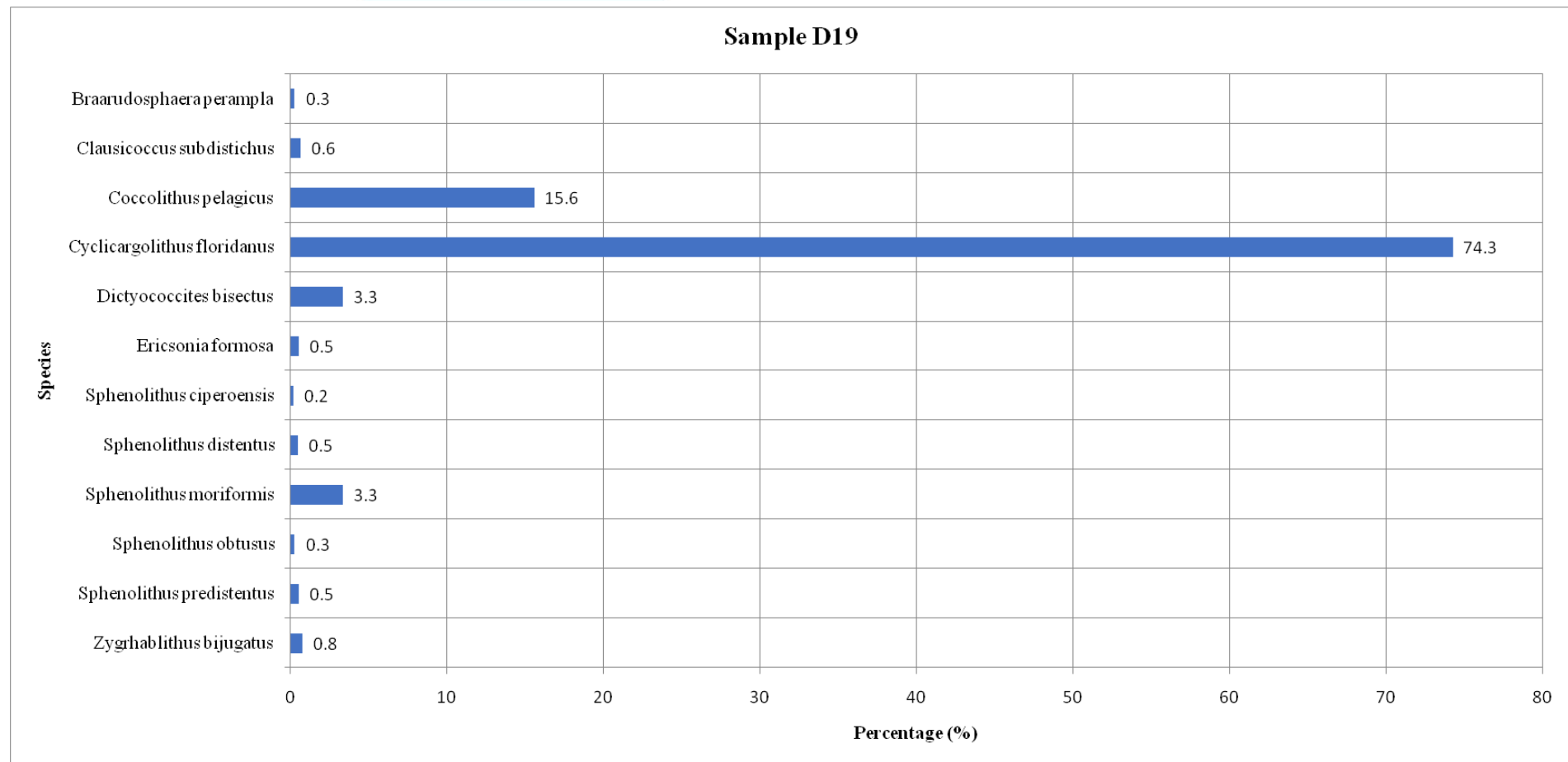
**Table 5.18 Species and number of specimens found in 300 FOV in sample D19.**

<b>D19</b>	
<b>Species</b>	<b>Specimens / 300 FOV</b>
<i>Braarudosphaera perampla</i>	1
<i>Coccolithus pelagicus</i>	61
<i>Cyclicargolithus floridanus</i>	291
<i>Dictyococcites bisectus</i>	13
<i>Ericsonia formosa</i>	2

**Table 5.19 Additional species and number of specimens found in 1500 FOV in sample D19.**

<b>D19</b>	
<b>Species</b>	<b>Specimens / 1500 FOV</b>
<i>Clausicoccus subdistichus</i>	12
<i>Sphenolithus ciperoensis</i>	3
<i>Sphenolithus distentus</i>	9





**Figure 5.11 Participation percentages of nannofossil species in the whole smear slide of sample D19.**

### Sample D29

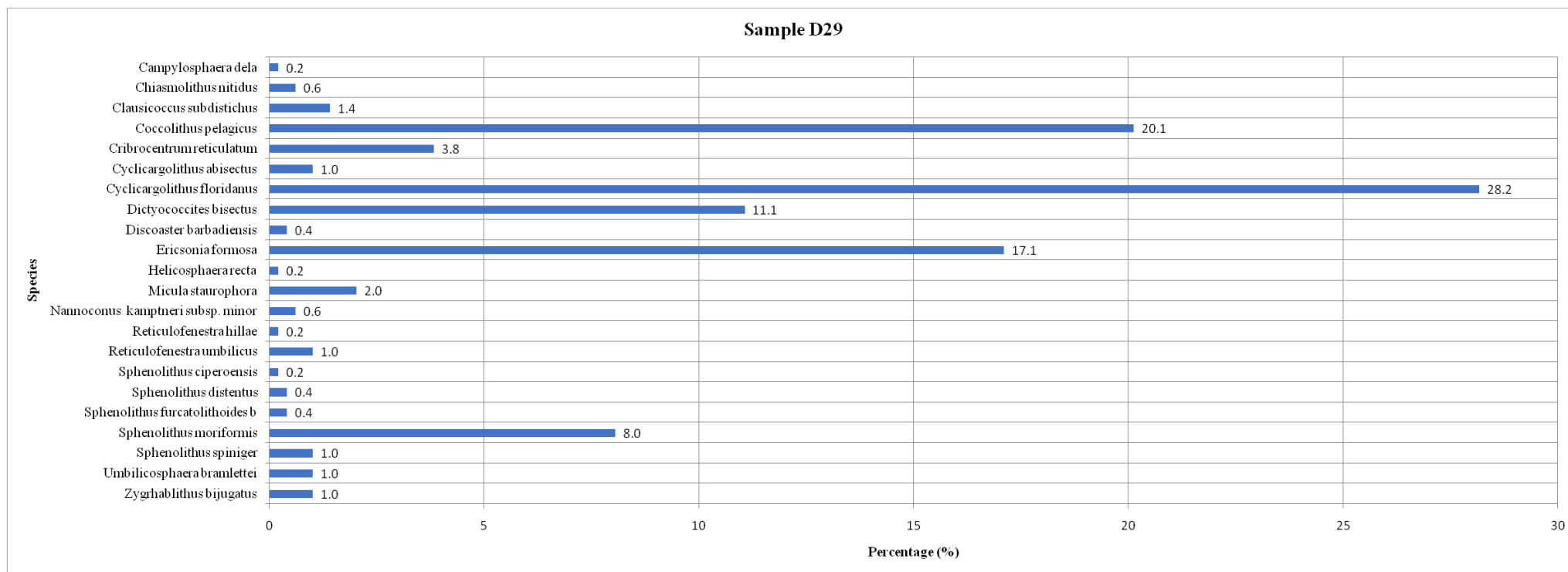
For sample D29 one smear slide has been studied under polarized light microscope. On Table 5.20 are shown the number of individual specimens of each species found in 3 traverses (300 FOV), randomly spanned across the smear slide. On Table 5.21, are shown the number of individual specimens of additional species found in the whole sample (1500 FOV). Finally, Figure 5.12 is a diagram showing the participation percentages of all species in the total nannofossil assemblage of sample D29.

**Table 5.20 Species and number of specimens found in 300 FOV in sample D29.**

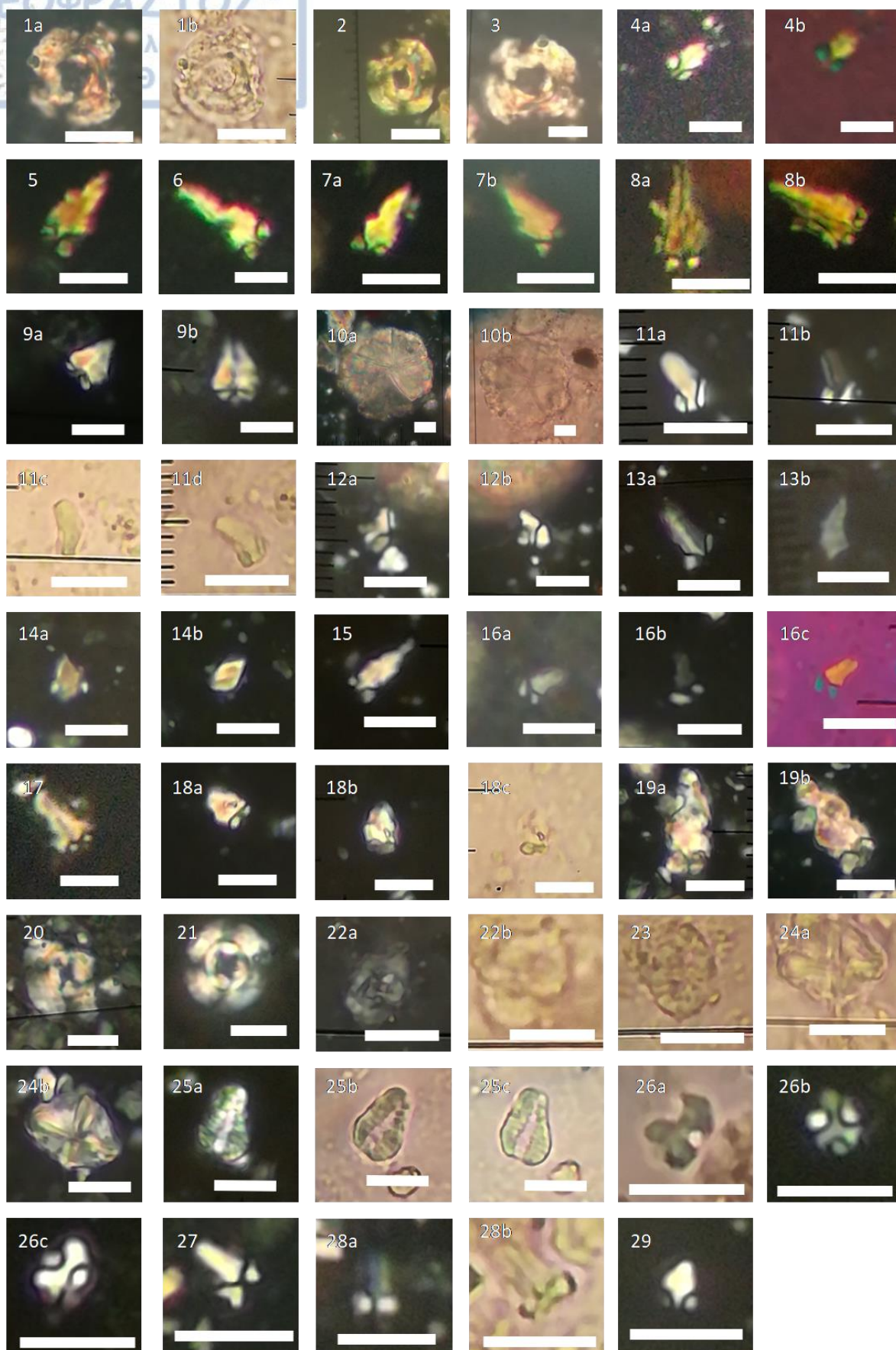
D29	
Species	Specimens / 300 FOV
<i>Coccolithus pelagicus</i>	20
<i>Cyclicargolithus abisectus</i>	1
<i>Cyclicargolithus floridanus</i>	28
<i>Dictyococcites bisectus</i>	11
<i>Ericsonia formosa</i>	17
<i>Micula staurophora</i>	2
<i>Reticulofenestra umbilicus</i>	1
<i>Sphenolithus moriformis</i>	8
<i>Sphenolithus spiniger</i>	1
<i>Zygrhablithus bijugatus</i>	1

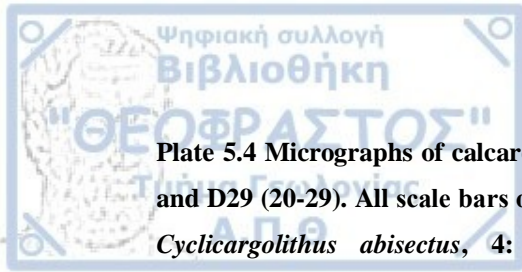
**Table 5.21 Additional species and number of specimens found in 1500 FOV in sample D29.**

D29	
Species	Specimens / 1500 FOV
<i>Campylosphaera dela</i>	1
<i>Chiasmolithus nitidus</i>	3
<i>Clausicoccus subdistichus</i>	7
<i>Cribrocentrum reticulatum</i>	19
<i>Discoaster barbadiensis</i>	2
<i>Helicosphaera recta</i>	1
<i>Nannoconus kamptneri subsp. minor</i>	3
<i>Reticulofenestra hillae</i>	1
<i>Sphenolithus ciperoensis</i>	1
<i>Sphenolithus distentus</i>	2
<i>Sphenolithus furcatolithoides "morphotype B"</i>	2
<i>Umbilicosphaera bramlettei</i>	5



**Figure 5.12 Participation percentages of nannofossil species in the whole smear slide of sample D29.**





**Plate 5.4** Micrographs of calcareous nannofossil species found in samples D18 (1-9), D19 (10-19) and D29 (20-29). All scale bars on bottom right of each photograph represent length of 5μm. 1-3: *Cyclicargolithus abisectus*, 4: *Sphenolithus ciperoensis*, 5-7: *Sphenolithus distentus*, 8-9: *Sphenolithus predistentus*, 10: *Braarudosphaera perampla*, 11: *Sphenolithus ciperoensis*, 13-16: *Sphenolithus distentus*, 17-19: *Sphenolithus predistentus*, 20-21: *Cyclicargolithus abisectus*, 22-23: *Helicosphaera recta*, 24: *Micula staurophora*, 25: *Nannoconus kamptneri* subsp. *minor*, 26: *Sphenolithus ciperoensis*, 27-29: *Sphenolithus distentus*.



## 6. Discussion / Biostratigraphical characterization

### 6.1 Chorafaki formation

#### Sample D16F

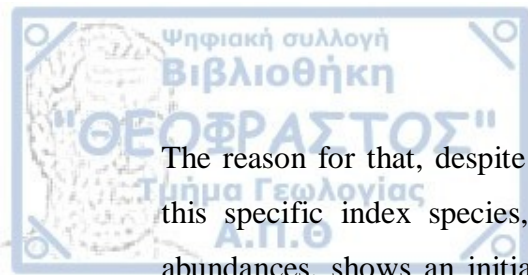
In the calcareous nannofossil assemblage identified in sample D16F no index species were found whose biohorizons could determine a specific biozone. However, its biostratigraphical characterization was possible by the absence of specific index species.

First of all, the coexistence of *Dictyococcites bisectus*, *Cribrrocentrum reticulatum*, *Coccolithus eopelagicus*, *Reticulofenestra hillae* and *Reticulofenestra umbilicus* indicate a range between the top of biozone NP16 and the undividable biozones NP19/20. Martini's biozonation shows uncertainties in defining the boundaries of biozones NP16-NP17, NP17-NP18 and NP19-NP20. This problem can be solved by advising the new biozones proposed by Agnini et al., 2014.

Agnini et al. (2014) have divided this interval into five separate biozones:

- CNE15, defined as the *Dictyococcites bisectus* / *Sphenolithus obtusus* concurrent range zone, between the Base of *Dictyococcites bisectus* and the Top of *Sphenolithus obtusus*.
- CNE16, defined as the *Chiasmolithus grandis* partial range zone, between the Top of *Sphenolithus obtusus* and the Base common of *Cribrrocentrum erbae*.
- CNE17, defined as the *Cribrrocentrum erbae* taxon range zone.
- CNE18, defined as the *Isthmolithus recurvus* partial range zone, between the Top common of *Cribrrocentrum erbae* and the Base of *Cribrrocentrum isabellae*.
- CNE19, defined as the *Cribrrocentrum isabellae* / *Cribrrocentrum reticulatum* concurrent range zone, between the Base of *Cribrrocentrum isabellae* and the Top of *Cribrrocentrum reticulatum*.

In sample D16F, there is total absence of the species *Sphenolithus obtusus*, *Chiasmolithus grandis*, *Cribrrocentrum erbae*, *Isthmolithus recurvus* and *Cribrrocentrum isabellae* placing it between the Top of *Cribrrocentrum erbae* and the Base common of *Isthmolithus recurvus*.



The reason for that, despite the fact that *Isthmolithus recurvus* is absent, is because this specific index species, according to higher resolution studies of *I. recurvus* abundances, shows an initial temporary and short-lived occurrence in Chron C17n, followed by an absence interval prior to the reentry of continuous (Base common) *I. recurvus* (Backman 1987, Catanzariti et al. 1997, Villa et al. 2008, Fornaciari et al. 2010).

Consequently, sample D16F has been determined to belong in the lower part of biozone CNE18 (Agnini et al., 2014) or NP18 (Martini, 1971) dating it between 36.9 Ma and 37.4 Ma.

The “in situ” calcareous nannofossil assemblage of sample D16F is represented by the species *Chiasmolithus nitidus*, *Clausicoccus subdistichus*, *Coccolithus eopelagicus*, *Coccolithus pelagicus*, *Cribrocentrum reticulatum*, *Cyclicargolithus floridanus*, *Dictyococcites bisectus*, *Discoaster nodifer*, *Ericsonia formosa*, *Neococcolithes dubius*, *Pontosphaera obliquipons*, *Reticulofenestra dictyoda*, *Reticulofenestra hillae*, *Reticulofenestra minuta*, *Reticulofenestra umbilicus*, *Sphenolithus moriformis*, *Sphenolithus radians*, *Umbilicosphaera bramlettei* and *Zygrabolithus bijugatus*.

Reworked species that have been found were *Blackites clavus*, *Campylosphaera dela*, *Chiasmolithus nitidus*, *Discoaster distinctus*, *Nannoconus funiculus*, *Sphenolithus furcatolithoides* “morphotype A” / “morphotype B” and *Sphenolithus spiniger*.

**Table 6.1 Calcareous nannofossil distribution for sample D16F based on the semi-quantitative analysis and the biostratigraphical characterization (P: Present, R: Rare, C: Common and RW: Reworked).**

Sample D16F	
Species	Distribution
<i>Coccolithus pelagicus</i>	C
<i>Cyclicargolithus floridanus</i>	C
<i>Ericsonia formosa</i>	C
<i>Chiasmolithus nitidus</i>	C
<i>Clausicoccus subdistichus</i>	R
<i>Cribocentrum reticulatum</i>	R
<i>Dictyococcites bisectus</i>	R
<i>Discoaster nodifer</i>	R
<i>Reticulofenestra dictyoda</i>	R
<i>Reticulofenestra hillae</i>	R
<i>Reticulofenestra minuta</i>	R
<i>Reticulofenestra umbilicus</i>	R
<i>Sphenolithus moriformis</i>	R
<i>Sphenolithus radians</i>	R
<i>Zygrhablithus bijugatus</i>	R
<i>Coccolithus eopelagicus</i>	P
<i>Neococcolithes dubius</i>	P
<i>Pontosphaera obliquipons</i>	P
<i>Umbilicosphaera bramlettei</i>	P
<i>Blackites clavus</i>	RW
<i>Campylosphaera dela</i>	RW
<i>Discoaster distinctus</i>	RW
<i>Nannoconus funiculus</i>	RW
<i>Sphenolithus furcatolithoides "morphotype A"</i>	RW
<i>Sphenolithus furcatolithoides "morphotype B"</i>	RW
<i>Sphenolithus spiniger</i>	RW

Noteworthy observations that derive from the age determination of sample D16F is the presence with high percentage of the reworked species *Sphenolithus furcatolithoides* and *Sphenolithus spiniger* as well as the fact that defining biozone NP18 for the base of Chorafaki formation is in agreement with previous biostratigraphical study carried out by Papanikolaou and Triantaphyllou (2010).

According to this study the base of Kirki formation has been determined as the lower part of biozone NP17 according to Martini (1971) or the top of CNE15 according to Agnini et al. (2014) due to the presence of *Sphenolithus obtusus*.

## 6.2 Avas formation

### Sample D26a

In the calcareous nannofossil assemblage identified in sample D26a, the index species *Isthmolithus recurvus* is sufficiently represented which indicates that biostratigraphically D26a is above the Base common of *Isthmolithus recurvus*. This fact along with the coexistence of *Discoaster barbadiensis*, *Discoaster saipanensis* and *Cribozentrum reticulatum* defines that D26a belongs to the indivisible zones NP19/NP20 (Martini, 1971).

Agnini et al. (2014), by considering as biohorizons the Base of *Cribozentrum isabellae* and the Top of *Cribozentrum reticulatum*, have divided the interval of NP19/20 biozones into three new zones:

- CNE18 which is defined as the *Isthmolithus recurvus* partial range zone, between the Top common of *Cribozentrum erbae* and the Base of *Cribozentrum isabellae*.
- CNE19 defined as the *Cribozentrum reticulatum*/*Cribozentrum isabellae* concurrent range zone, between the Base of *C. isabellae* and the Top of *C. reticulatum*.
- CNE20 defined as the Top zone of *Discoaster saipanensis*, between the Top of *C. reticulatum* and the Top of *D. saipanensis*.

In the assemblage of sample D26a *Cribozentrum isabellae* was absent, thus concluding that D26a is placed between the Base common of *I. recurvus* and the Base of *C. isabellae*.

Consequently, sample D26a (base of Avas formation) has been determined to belong in the upper part of biozone CNE18 (Agnini et al., 2014) or low NP19/NP20 (Martini, 1971) dating it between 36.2 Ma and 36.9 Ma.

The “in situ” calcareous nannofossil assemblage of sample D26a is represented by the species *Braarudosphaera bigelowii*, *Chiasmolithus oamaruensis*, *Coccolithus*

*eopelagicus*, *Coccolithus pelagicus*, *Cribrocentrum reticulatum*, *Cyclicargolithus floridanus*, *Dictyococcites bisectus*, *Discoaster barbadiensis*, *Discoaster saipanensis*, *Ericsonia formosa*, *Isthmolithus recurvus*, *Pontosphaera multipora*, *Pontosphaera obliquipons*, *Pontosphaera plana*, *Reticulofenestra dictyoda*, *Reticulofenestra hillae*, *Reticulofenestra umbilicus*, *Sphenolithus moriformis*, *Umbilicosphaera bramlettei*, *Zygrhablithus bijugatus* and *Zygrhablithus bijugatus* subsp. *cornutus*.

Reworked species that have been found were *Braarudosphaera insecta*, *Pontosphaera ocellata* and *Sphenolithus obtusus*.

**Table 6.2** Calcareous nannofossil distribution for sample D26a based on the semi-quantitative analysis and the biostratigraphical characterization (P: Present, R: Rare, C: Common and RW: Reworked).

Sample D26a	
Species	Distribution
<i>Coccolithus pelagicus</i>	C
<i>Dictyococcites bisectus</i>	C
<i>Zygrhablithus bijugatus</i>	C
<i>Braarudosphaera bigelowii</i>	C
<i>Cribrocentrum reticulatum</i>	R
<i>Cyclicargolithus floridanus</i>	R
<i>Discoaster saipanensis</i>	R
<i>Ericsonia formosa</i>	R
<i>Isthmolithus recurvus</i>	R
<i>Reticulofenestra dictyoda</i>	R
<i>Sphenolithus moriformis</i>	R
<i>Umbilicosphaera bramlettei</i>	R
<i>Chiasmolithus oamaruensis</i>	P
<i>Coccolithus eopelagicus</i>	P
<i>Discoaster barbadiensis</i>	P
<i>Pontosphaera multipora</i>	P
<i>Pontosphaera obliquipons</i>	P
<i>Pontosphaera plana</i>	P
<i>Reticulofenestra hillae</i>	P
<i>Reticulofenestra umbilicus</i>	P
<i>Zygrhablithus bijugatus</i> subsp. <i>cornutus</i>	P
<i>Braarudosphaera insecta</i>	RW
<i>Pontosphaera ocellata</i>	RW
<i>Sphenolithus obtusus</i>	RW



### 6.3 Pylaea formation

#### Sample D20

In the assemblage of sample D20, the coexistence of the species *Helicosphaera recta* and *Cyclicargolithus abisectus* as well as the absence of *Reticulofenestra umbilicus* strongly indicates that sample D20 belongs in biozone NP23.

This is further endorsed by the presence of the species *Sphenolithus tawfikii* which has its Base in NP23. The species *S. tawfikii* is a species of the genus *Sphenolithus* that has been introduced and described by Bergen et al. (2017). Aside from Bergen et al., 2019 no further references have been found considering this species making it not well established. The found specimens, though, show great resemblances to its description and so have been identified as such.

Additionally in the assemblage of sample D20 occur rare specimens of the genus *Sphenolithus* that show an intermediate morphology between *S. predistentus* and *S. distentus*. This fact matches the remarks by Agnini et al 2014 considering the assemblages for biozone CNO3 and in the present research these specimens are mentioned as “*Sphenolithus distentus* ?”.

To conclude, sample D20 has been determined to belong in lower biozone NP23 (Martini, 1971) or lower CNO3 (Agnini et al., 2014) dating it between 31 Ma and 32 Ma.

The “in situ” calcareous nannofossil assemblage of sample D20 is represented by the species *Clausicoccus subdistichus*, *Coccolithus pelagicus*, *Cyclicargolithus abisectus*, *Cyclicargolithus floridanus*, *Dictyococcites bisectus*, *Helicosphaera recta*, *Sphenolithus akropodus*, *Sphenolithus distentus*, *Sphenolithus moriformis*, *Sphenolithus predistentus*, *Sphenolithus tawfikii* and *Zygrhablithus bijugatus*.

Reworked species that have been found were *Criboecium reticulatum*, *Ericsonia formosa*, *Micula staurophora*, *Pontosphaera punctosa*, *Sphenolithus obtusus* and *Sphenolithus spiniger*.

**Table 6.3** Calcareous nannofossil distribution for sample D20 based on the semi-quantitative analysis and the biostratigraphical characterization (P: Present, R: Rare, C: Common and RW: Reworked).

Sample D20	
Species	Distribution
<i>Cyclicargolithus floridanus</i>	C
<i>Zygrhablithus bijugatus</i>	C
<i>Coccolithus pelagicus</i>	C
<i>Dictyococcites bisectus</i>	R
<i>Helicosphaera recta</i>	R
<i>Sphenolithus moriformis</i>	R
<i>Clausicoccus subdistichus</i>	P
<i>Cyclicargolithus abisectus</i>	P
<i>Sphenolithus distentus</i> ?	P
<i>Sphenolithus predistentus</i>	P
<i>Sphenolithus akropodus</i>	RW
<i>Cribrocentrum reticulatum</i>	RW
<i>Ericsonia formosa</i>	RW
<i>Micula staurophora</i>	RW
<i>Pontosphaera punctosa</i>	RW
<i>Sphenolithus furcatolithoides</i> "morphotype B"	RW
<i>Sphenolithus obtusus</i>	RW
<i>Sphenolithus spiniger</i>	RW

### **Sample D24**

In the identified calcareous nannoplankton assemblage of sample D24 the species *Sphenolithus tawfikii* is present while *Sphenolithus distentus* is totally absent. By taking into consideration, also, that sample D24 is stratigraphically higher than sample D20 it can be concluded that sample D24 belongs in lower Zone NP23 (Martini, 1971) or upper Zone CNO3 (Agnini et al., 2014) dating it between 30 Ma and 31 Ma.

The “in situ” calcareous nannofossil assemblage of sample D24 is represented by the species *Coccolithus pelagicus*, *Cyclicargolithus floridanus*, *Dictyococcites bisectus*, *Sphenolithus moriformis*, *Sphenolithus tawfikii* and *Zygrhablithus bijugatus*.

Reworked species that have been found were *Ericsonia formosa*, *Isthmolithus recurvus*, *Reticulofenestra hillae* and *Reticulofenestra umbilicus*.

**Table 6.4** Calcareous nannofossil distribution for sample D24 based on the semi-quantitative analysis and the biostratigraphical characterization (P: Present, R: Rare, C: Common and RW: Reworked).

Sample D24	
Species	Distribution
<i>Coccolithus pelagicus</i>	C
<i>Cyclicargolithus floridanus</i>	R
<i>Dictyococcites bisectus</i>	R
<i>Sphenolithus moriformis</i>	R
<i>Sphenolithus tawfikii</i>	P
<i>Zygrhablithus bijugatus</i>	P
<i>Ericsonia formosa</i>	RW
<i>Isthmolithus recurvus</i>	RW
<i>Reticulofenestra hillae</i>	RW
<i>Reticulofenestra umbilicus</i>	RW

#### **Samples D28B, D28a, D27 and D17B**

The calcareous nannofossil assemblages of samples D28B, D28a, D27 and D17B are all characterized by the coexistence of *Sphenolithus predistentus* and *Sphenolithus distentus* while also the absence of *Sphenolithus ciperoensis* indicating that they belong in upper Zone NP23 (Martini, 1971) or CNO4 (Agnini et al., 2014) which is the *S. predistentus*/*S. distentus* Concurrent Range Zone dating it between 27,2 Ma and 30 Ma.

The “in situ” calcareous nannofossil assemblage of sample D28B is represented by the species *Coccolithus pelagicus*, *Cyclicargolithus floridanus*, *Dictyococcites bisectus*, *Sphenolithus distentus*, *Sphenolithus moriformis*, *Sphenolithus predistentus* and *Sphenolithus tawfikii*.

Reworked species that have been found were *Ericsonia formosa* and *Sphenolithus obtusus*.

For sample D28a the “in situ” assemblage is represented by *Cyclicargolithus floridanus*, *Dictyococcites bisectus*, *Sphenolithus distentus*, *Sphenolithus moriformis*, *Sphenolithus predistentus*, *Sphenolithus tawfikii*.



Reworked species that have been found were *Ericsonia formosa* and *Umbilicosphaera bramlettei*.

For sample D27 the “in situ” assemblage is represented by the species *Coccolithus pelagicus*, *Cyclicargolithus floridanus*, *Dictyococcites bisectus*, *Sphenolithus distentus*, *Sphenolithus predistentus* and *Sphenolithus tawfikii*.

Reworked species that have been found were *Ericsonia formosa* and *Reticulofenestra hillae*.

The “in situ” calcareous nannofossil assemblage of sample D17B is represented by the species *Braarudosphaera bigelowii*, *Clausicoccus subdistichus*, *Coccolithus pelagicus*, *Cyclicargolithus abisectus*, *Cyclicargolithus floridanus*, *Dictyococcites bisectus*, *Sphenolithus distentus*, *Sphenolithus moriformis*, *Sphenolithus predistentus*, *Sphenolithus tawfikii*, *Zygrhablithus bijugatus*.

Reworked species that have been found were *Ericsonia formosa*.

**Table 6.5** Calcareous nannofossil distribution for samples D28B, D28a, D27 and D17B based on the semi-quantitative analysis and the biostratigraphical characterization (P: Present, R: Rare, C: Common and RW: Reworked).

Species	Samples			
	D28B	D28a	D27	D17B
<i>Cyclicargolithus floridanus</i>	C	C	R	C
<i>Dictyococcites bisectus</i>	R	R	R	C
<i>Coccolithus pelagicus</i>	C		R	R
<i>Sphenolithus moriformis</i>	R	R		R
<i>Zygrhablithus bijugatus</i>				R
<i>Braarudosphaera bigelowii</i>				P
<i>Clausicoccus subdistichus</i>				P
<i>Cyclicargolithus abisectus</i>				P
<i>Sphenolithus distentus</i>	P	P	P	P
<i>Sphenolithus predistentus</i>	P	P	P	P
<i>Sphenolithus tawfikii</i>	P	P	P	P
<i>Sphenolithus obtusus</i>	RW			
<i>Ericsonia formosa</i>	RW	RW	RW	RW

### Samples D18 and D19

Samples D18 and D19 show similar assemblages, characterized by the coexistence of the index species *Sphenolithus predistentus*, *S. distentus* and *S. ciperoensis*. Martini (1971) has defined the interval when these three species coexist as Zone NP24, a concurrent range zone from the Base of *S. ciperoensis* until the Top of *S. distentus*, with the Top of *S. predistentus* occurring in between them. However, Agnini et al. (2014) have disregarded this zone as inconsistent due to the fact that the biohorizons used (Base of *S. ciperoensis* and Top of *S. distentus*) occur slightly below and above the Top of *S. predistentus*. In contrast, in Agnini et al. (2014) biozonation, for the same interval, only the Top of *S. predistentus* is used as a biohorizon that separates zones CNO4 (*S. distentus*/*S. predistentus* CRZ) and CNO5 (*S. ciperoensis* TZ) while also mentioning that “in upper Zone CNO4 specimens with intermediate morphology between *S. ciperoensis* and *S. distentus* become present before the genuine *Sphenolithus ciperoensis* is established (Olafsson & Villa, 1992; Blaj et al., 2009).”

The specimens of *Sphenolithus ciperoensis* found in samples D18 and D19 are badly preserved therefore it can't be said with certainty whether they are genuine *S. ciperoensis* or the intermediate morphotypes that Agnini et al. (2014) have described. In either case, these specimens along with the presence of *S. predistentus* and *S. distentus* indicate that samples D18 and D19 belong to Zone NP24 (Martini, 1971) or upper Zone CNO4 (Agnini et al., 2014) dating it between 27 Ma and 27,2 Ma.

The “in situ” calcareous nannofossil assemblage of sample D18 is represented by the species *Clausicoccus subdistichus*, *Coccolithus pelagicus*, *Cyclicargolithus abisectus*, *Cyclicargolithus floridanus*, *Dictyococcites bisectus*, *Discoaster deflandrei*, *Helicosphaera compacta*, *Sphenolithus ciperoensis*, *Sphenolithus distentus*, *Sphenolithus predistentus* and *Zygrhablithus bijugatus*.

Reworked species that have been found were *Coccolithus eopelagicus*, *Ericsonia formosa*, *Pontosphaera plana*, *Pontosphaera pulchra*, *Reticulofenestra umbilicus* and *Sphenolithus obtusus*.

The “in situ” calcareous nannofossil assemblage of sample D19 is represented by the species *Braarudosphaera perampla*, *Clausicoccus subdistichus*, *Coccolithus*



*pelagicus*, *Cyclicargolithus floridanus*, *Dictyococcites bisectus*, *Sphenolithus ciproensis*, *Sphenolithus distentus*, *Sphenolithus moriformis*, *Sphenolithus predistentus* and *Zygrhablithus bijugatus*.

Reworked species that have been found were *Ericsonia formosa* and *Sphenolithus obtusus*.

**Table 6.6** Calcareous nannofossil distribution for samples D18 and D19 based on the semi-quantitative analysis and the biostratigraphical characterization (P: Present, R: Rare, C: Common and RW: Reworked).

Species	Samples	
	D18	D19
<i>Braarudosphaera perampla</i>		P
<i>Clausicoccus subdistichus</i>	R	R
<i>Coccolithus pelagicus</i>	C	C
<i>Cyclicargolithus abisectus</i>	P	
<i>Cyclicargolithus floridanus</i>	C	C
<i>Dictyococcites bisectus</i>	R	R
<i>Discoaster deflandrei</i>	R	
<i>Helicosphaera compacta</i>	P	
<i>Sphenolithus ciproensis</i>	P	P
<i>Sphenolithus distentus</i>	P	P
<i>Sphenolithus moriformis</i>	C	R
<i>Sphenolithus predistentus</i>	P	P
<i>Zygrhablithus bijugatus</i>	C	P
<i>Coccolithus eopelagicus</i>	RW	
<i>Ericsonia formosa</i>	RW	RW
<i>Pontosphaera plana</i>	RW	
<i>Pontosphaera pulchra</i>	RW	
<i>Reticulofenestra umbilicus</i>	RW	
<i>Sphenolithus obtusus</i>	RW	RW

### Sample D29

Sample D29 is from the upper part of the Pylaea formation. Its assemblage is characterized by intense reworking with the presence of reworked species that

resembles the assemblage of sample D16F like *Sphenolithus furcatolithoides* "morphotype B" and Cretaceous species (*Micula staurophora*, *Nannoconus kamptneri*). Concerning the index species, *Sphenolithus distentus* and *S. ciperoensis* were present while *Sphenolithus predistentus* was absent. Similarly with samples D18 and D19 the rare specimens of *S. distentus* are not considered reworked therefore the age of sample D29 should be below the Top of *S. distentus*. Along with the presence of *S. ciperoensis*, the absence of *S. predistentus* as well as the fact that sample D29 is stratigraphically higher than samples D18 and D19 it is concluded that sample D29 belongs to Zone NP24 (Martini, 1971) or lower CNO5 (Agnini et al., 2014) dating it between 26,8 Ma and 27 Ma.

The "in situ" calcareous nannofossil assemblage of sample D29 is represented by the species *Chiasmolithus nitidus*, *Clausicoccus subdistichus*, *Coccolithus pelagicus*, *Cyclicargolithus abisectus*, *Cyclicargolithus floridanus*, *Dictyococcites bisectus*, *Helicosphaera recta*, *Sphenolithus ciperoensis*, *Sphenolithus distentus*, *Sphenolithus moriformis*, *Zygrhablithus bijugatus*.

Reworked species that have been found were *Campylosphaera dela*, *Cribrocentrum reticulatum*, *Discoaster barbadiensis*, *Ericsonia formosa*, *Micula staurophora*, *Nannoconus kamptneri* subsp. *minor*, *Reticulofenestra hillae*, *Reticulofenestra umbilicus*, *Sphenolithus furcatolithoides* "morphotype B", *Sphenolithus spiniger* and *Umbilicosphaera bramlettei*.

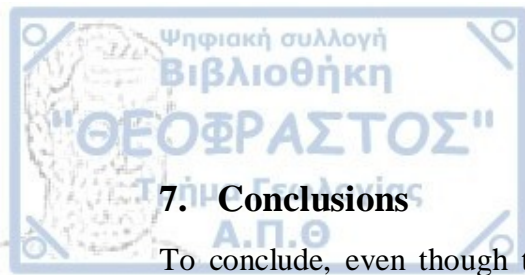
**Table 6.7** Calcareous nannofossil distribution for sample D29 based on the semi-quantitative analysis and the biostratigraphical characterization (P: Present, R: Rare and RW: Reworked).

Sample D29	
Species	Distribution
<i>Chiasmolithus nitidus</i>	<b>R</b>
<i>Clausicoccus subdistichus</i>	<b>R</b>
<i>Coccolithus pelagicus</i>	<b>R</b>
<i>Cyclicargolithus floridanus</i>	<b>R</b>
<i>Dictyococcites bisectus</i>	<b>R</b>
<i>Sphenolithus moriformis</i>	<b>R</b>
<i>Cyclicargolithus abisectus</i>	<b>P</b>
<i>Helicosphaera recta</i>	<b>P</b>
<i>Sphenolithus ciperoensis</i>	<b>P</b>
<i>Sphenolithus distentus</i>	<b>P</b>
<i>Zygrhablithus bijugatus</i>	<b>P</b>
<i>Campylosphaera dela</i>	<b>RW</b>
<i>Cribocentrum reticulatum</i>	<b>RW</b>
<i>Discoaster barbadiensis</i>	<b>RW</b>
<i>Ericsonia formosa</i>	<b>RW</b>
<i>Micula staurophora</i>	<b>RW</b>
<i>Nannoconus kamptneri subsp. minor</i>	<b>RW</b>
<i>Reticulofenestra hillae</i>	<b>RW</b>
<i>Reticulofenestra umbilicus</i>	<b>RW</b>
<i>Sphenolithus furcatolithoides "morphotype B"</i>	<b>RW</b>
<i>Sphenolithus spiniger</i>	<b>RW</b>
<i>Umbilicosphaera bramlettei</i>	<b>RW</b>

Finally, in Figure 6.1 is a chart summarizing the results along with the biostratigraphical characterization. It features a simplified stratigraphic column of the Alexandroupolis sub-basin (not in scale), the analyzed samples in their stratigraphic position, index nannofossil species which were found in their assemblages, the adjusted biozones according to both schemes by Martini (1971) and Agnini et al. (2014) and eventually the determined age range.

Chronostratigraphy		Alexandroupolis sub-basin Stratigraphic column (Western Thrace)	Samples	Biozones		Age (Ma)	Calcareous Nannofossils																											
				Martini 1971	Agnini et al. 2014		<i>Cyclicargolithus floridanus</i>	<i>Sphenolithus moriformis</i>	<i>Zygababidius bijugatus</i>	<i>Isthmolithus recurvus</i>	<i>Chiasmolithus oamaruensis</i>	<i>Cribrocentrum reticulatum</i>	<i>Clausicoccus subdistichus</i>	<i>Discoaster barbadensis</i>	<i>Discoaster saipanensis</i>	<i>Ericsonia formosa</i>	<i>Helicosphaera bramlettei</i>	<i>Helicosphaera compacta</i>	<i>Reticulococites bisectus</i>	<i>Reticulofenestra hillae</i>	<i>Coccolithus eopelagicus</i>	<i>Sphenolithus umbilicus</i>	<i>Sphenolithus tawfikii</i>	<i>Cyclicargolithus akropodus</i>	<i>Helicosphaera abisectus</i>	<i>Sphenolithus recta</i>	<i>Sphenolithus predistans</i>	<i>Sphenolithus distans</i>	<i>Sphenolithus ciperoensis</i>					
OLIGOCENE	LATE	?	Fere Fm	D29	?	?	26,8-27																											
		Pylaea Fm	NP24		CNO5																													
		Tuffs																																
		Pylaea Fm			CNO4	27-27,2																												
		Tuffs				27,2-30																												
						27,2-30																												
	EARLY		D18, D19			D17B		D27	NP23	27,2-30																								
		27,2-30																																
		27,2-30																																
	EOCENE	MIDDLE	LATE		D28a D28B D24	D20		CNO3	30-31																									
									31-32																									
?				?																														
NP19/20				CNE18			36,2-36,9																											
NP18							36,9-37,4																											
EOCENE	MIDDLE	LATE	D26a	D16F	?	?	NP17	CNE15																										

Figure 6.1 Chart showing the final results and the biostratigraphic interpretation of the samples that contained nannofossils and have been analyzed in this study.



## 7. Conclusions

To conclude, even though the low preservation of calcareous nannofossils and the intense reworking proved to be a challenging factor, the biostratigraphical characterization of the Paleogene molassic formations which comprise the Alexandroupolis sub-basin has been achieved.

All samples from the stratigraphically lowest molassic formations including the flysch of Melia Fm, Kirki Fm and the Sandstone member were barren of nannofossils rendering it unable to determine a biozone for them.

The formations of Chorafaki Fm and the base of Avas Fm have been determined to be of Late Eocene age, the Lower part of Pylaea Fm of Early Oligocene age and the upper part of Pylaea of Late Oligocene.

The exact Eocene - Oligocene boundary could not be determined as there appears to be a lack of nannofossil data from the base of Avas Fm until the base of Pylaea Fm. This “hiatus” lasts for approximately 4 Ma and could be translated as the period during which the carbonatic platform was active depositing the neritic limestones of Avas Fm.



## 8. References

- Agnini, C., Fornaciari, E., Raffi, I., Catanzariti, R., Pälike, H., Backman, J., et al. (2014). Biozonation and biochronology of Paleogene calcareous nannofossils from low and middle latitudes. *Newsletters on Stratigraphy* , 47, pp. 131–181.
- Agnini, C., Monechi, S., & Raffi, I. (2017). Calcareous nannofossil biostratigraphy: historical background and application in Cenozoic chronostratigraphy. *Lethaia* (50), pp. 447-463.
- Backman, J. (1987). Quantitative calcareous nannofossil biocronology of middle Eocene through early Oligocene sediments from DSDP Sites 522 and 523. *Abhandlungen Geologischen Bundesanstalt* , 39, pp. 21-31.
- Backman, J., & Shackleton, N. (1983). Quantitative biochronology of Pliocene and early Pleistocene calcareous nannoplankton from the Atlantic, Indian and Pacific Oceans. *Marine Micropaleontology* , 8, pp. 141-170.
- Backman, J., Raffi, I., Rio, D., Fornaciari, E., & Pälike, H. (2012). Biozonation and biochronology of Miocene through Pleistocene calcareous nannofossils from low and middle latitudes. *Newsletters on Stratigraphy* , 47.
- Bergen, J., de Kaenel, E., Blair, S., Boesiger, T., & Browning, E. (2017). Oligocene-Pliocene taxonomy and stratigraphy of the genus *Sphenolithus* in the circum North Atlantic Basin: Gulf of Mexico and ODP Leg 154. *Journal of Nannoplankton Research* , 37 (2-3), pp. 77-112.
- Bergen, J., De Kaenel, E., Blair, S., Browning, E., Lundquist, J., Boesiger, T., et al. (2019). BP Gulf of Mexico Neogene Astronomically-tuned Time Scale (BP GNATTS). *GSA Bulletin* , p. 131.
- Blaj, T., Backman, J., & Raffi, I. (2009). Late Eocene to Oligocene preservation history and biochronology of calcareous nannofossils from paleo-equatorial Pacific Ocean sediments. *Rivista Italiana di Paleontologia e Stratigrafia* , 115, pp. 67-85.
- Bown, P. (1998). Calcareous nannofossil biostratigraphy. *British Micropalaeontological Society Publication Series* , p. 328.

Bown, P., & Young, J. (1998). *Techniques*. In: Bown, P.R., Ed., *Calcareous Nannofossil Biostratigraphy (British Micropalaeontological Society Publications Series)*. London: Chapman and Kluwer Academic.

Bown, P., Cooper, M., & Lord, A. (1988, 12). A Calcareous Nannofossil Biozonation Scheme for the early to mid Mesozoic. *Newsletters on Stratigraphy* , 20 (2), pp. 91-114.

Catanzariti, R., Rio, D., & Martelli, L. (1997). Late Eocene to Oligocene calcareous nannofossil biostratigraphy in the northern Apennines: the Ranzano sandstone. *Memorie di Scienze Geologiche* , 49, pp. 207-253.

Christodoulou, G. (1958). Ueber das Alter einiger Formationen von Samothraki. *Bulletin of the Geological Society of Greece* , III/1, pp. 40–45.

Dragomanov, L., Grigorov, V., Ioncher, A., Jelev, A., & Darakchieva, S. (1986). Lithological indications of the presence of Middle Eocene in the Eastern Rhodopes. *Ann. Higher Inst. Mining Geol.* , 32, pp. 37–41.

Ducklow, H. (2001). Upper Ocean Carbon Export and the Biological Pump. *Oceanography* , 14, pp. 50-54.

Fornaciari, E., Agnini, C., Catanzariti, R., Rio, D., Bolla, E., & Valvasoni, E. (2010). Mid-latitude calcareous nannofossil biostratigraphy, biochronology and evolution across the middle to late Eocene transition. *Stratigraphy* , 7, pp. 229-264.

Görür, N., & Okay, A. (1996). A fore-arc origin for the Thrace Basin, NW Turkey. *International Journal of Earth Sciences.* , 85, pp. 662-668.

Jordan, R., & Chamberlain, A. (1997). Biodiversity among haptophyte algae. *Biodiversity and Conservation* , 6, pp. 131-152.

Kilias, A., Falalakis, G., Sfeikos, A., Papadimitriou, E., Vamvaka, A., & Gkarlaouni, C. (2013). The Thrace basin in the Rhodope province of NE Greece — A tertiary supradetachment basin and its geodynamic implications. *Tectonophysics* , 595-596, pp. 90-105.

Kopp, K. (1966). Geologie Thrakiens III: Das Tertiär zwischen Rhodope und Evros. *Ann. Geol. Pays Hellen* , 16, pp. 315-362.

Kopp, K., Pavoni, N., & Schindler, C. (1969). Geologie Thrakiens IV: Das Ergene Becken. *Beihefte Geol. Jahrbuch* 76 , p. 136 pp.

Maravelis, A., & Zelilidis, A. (2010). Petrography and geochemistry of the late Eocene–early Oligocene submarine fans and shelf deposits on Lemnos Island, NE Greece. Implications for provenance and tectonic setting. *Geological Journal* , 45 (4), pp. 412-433.

Martini, E. (1971). Standard Tertiary and Quaternary calcareous nannoplankton zonation. In: A. Farinacci (Ed.). *Proceedings of the Second International Conference on Planktonic Microfossils* , 2, p. 739–785.

Meinhold, G., & BonDagher-Fadel, M. (2010). Geochemistry and biostratigraphy of Eocene sediments from Samothraki island, NE Greece. *N. Jb. Geol. Palaeont. Abh.* , 256(1), pp. 17-38.

Milliman, J. (1993). Production and accumulation of calcium carbonate in the ocean: Budget of a nonsteady state. *Global Biogeochemical Cycles* , 7 (4), pp. 927-957.

Mountrakis, D. (2010). Geology and Geotectonic Evolution of Greece.

Okada, H., & Bukry, D. (1980). Supplementary modification and introduction of code numbers to the low-latitude coccolith biostratigraphic zonation (Bukry 1973, 1975). *Marine Micropaleontology* , 5, pp. 321–325.

Okay, A., Altiner, D., Sunal, G., Aygöl, M., Akdoğan, R., Altiner, S., et al. (2017, September 15). Geological evolution of the Central Pontides. In: Simmons M.D., Tari G.C. & Okay A.I. (eds) *Petroleum Geology of the Black Sea.* , p. 464.

Okay, A., Özcan, E., Hakyemez, A., Siyako, M., Sunal, G., & Kylander-Clark, A. (2019). The Thrace Basin and the Black Sea: The Eocene–Oligocene marine connection. *Geological Magazine* , 156(1), pp. 39-61.

Okay, A., Siyako, M., & Bürkan, K. (1990). Geology and tectonic evolution of the Biga Peninsula. *Turkish Association of Petroleum Geologists Bulletin* , 2, pp. 83-121.

Olafsson, G., & Villa, G. (1992). Reliability of sphenoliths as zonal markers in Oligocene sediments from the Atlantic and Indian Oceans. *Memorie Scienze Geologiche* , 43, pp. 261-275.

Özcan, E., Less, G., Okay, A., Báldi-Beke, M., Kollányi, K., & Yilmaz, I. (2010). Stratigraphy and larger Foraminifera of the Eocene shallow-marine and olistostromal units of the southern part of Thrace Basin, NW Turkey. *Turkish Journal of Earth Sciences* , 19, pp. 27-77.

Papanikolaou, D., & Triantaphyllou, M. (2010). Tectonostratigraphic observations in the western Thrace Basin in Greece and correlations with the eastern part in Turkey.

Perch-Nielsen, K. (1985). Cenozoic Calcareous Nannofossils. In: Bolli, H.M., Saunders, J.B. and Perch-Nielsen, K., Eds., *Plankton Stratigraphy* , pp. 329-426.

Roussos, N. (1994). Stratigraphic and paleogeographic evolution of the Paleogene Molassic basins of the Northern Aegean. *Bull. Geol. Soc. Greece* , 32, pp. 275-294.

Sarmiento, J., & Gruber, N. (2004, September 10). Ocean Biogeochemical Dynamics.

Siyako, M., & Huvaz, O. (2007). Eocene stratigraphic evolution of the Thrace Basin, Turkey. *Sedimentary Geology* , 198, pp. 75-91.

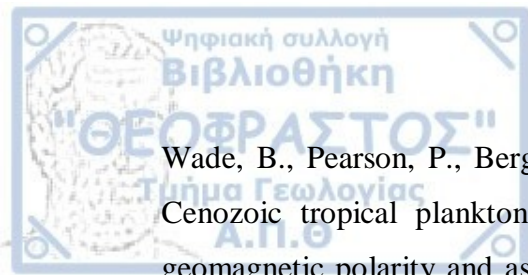
Tranos, M. (2009). Faulting of Lemnos Island; a mirror of faulting of the North Aegean Trough (northern Greece). *Tectonophysics* , 467 (1-4), pp. 72-88.

Tsirambides, A., Kassoli-Fournaraki, A., Filippidis, A., & Soldatos, K. (1989). Preliminary results on clinoptilolite-containing volcanoclastic sediments from Metaxades, NE Greece. *Bulletin of the Geological Society of Greece* , 23, pp. 451-460.

Turgut, S., & Eseller, G. (2000). Sequence stratigraphy, tectonics and depositional history in eastern Thrace Basin, NW Turkey. *Marine and Petroleum Geology* , 17, pp. 61-100.

Turgut, S., Turkaslan, M., & Perincek, D. (1991). Evolution of the Thrace sedimentary basin and its hydrocarbon prospectivity. In: Spencer AM (ed) *Generation, accumulation, and production of Europe's hydrocarbons. Spec Publ Eur Assoc Petrol* , pp. 415–437.

Villa, G., Fioroni, C., Pea, L., Bohaty, S., & Persico, D. (2008). Middle Eocene–late Oligocene climate variability: Calcareous nannofossil response at Kerguelen Plateau, Site 748. *Marine Micropaleontology* , 69, pp. 173-192.



Wade, B., Pearson, P., Berggren, W., & Pälike, H. (2011). Review and revision of Cenozoic tropical planktonic foraminiferal biostratigraphy and calibration to the geomagnetic polarity and astronomical time scale. *Earth-Science Reviews* , 104, pp. 111-142.

Young, J., Bown, P., & Lees, J. (2017, 1 20). Nannotax3 website. *International Nannoplankton Association* , p. <http://www.mikrotax.org/Nannotax3>.

Παπανικολάου, Ι. (2015). *Γεωλογία της Ελλάδας*. Πατακης.